CDX2 is Essential for Cell Proliferation and Polarity in Porcine Blastocysts

Authors: Gerelchimeg Bou,[1,2] Shichao Liu,[1] Mingju Sun,[1] Jiang Zhu,[1] Binghua Xue,[1] Jia Guo,[1] Yueming Zhao,[1] Bo Qu,[3] Xiaogang Weng,[1] Yanchang Wei,[1] Lei Lei,[4] Zhonghua Liu[1,5]

Affiliations:

[1]College of Life Science, Northeast Agricultural University, Harbin 150030, China

[2]College of Animal Science, Inner Mongolia Agricultural University, Huhhot 010018, China

[3]Life Science and Biotechnique Research Center, Northeast Agricultural University, Harbin 150030, China

[4]Department of Histology and Embryology, Harbin Medical University, Harbin 150081, China

[5]Key Laboratory of Animal Genetics, Breeding and Reproduction, Education Department of Heilongjiang Province, Harbin 150030, China

Correspondence to Zhonghua Liu: liuzhonghua@neau.edu.cn; liu086@yahoo.com

Key words: CDX2, TE polarity, Cell proliferation, BMP4, PKCα, Pig

Summary statement: A study of porcine embryos systematically illustrated a differential CDX2 expression and functional patterning in different mammalian embryos.

Abstract

The role of CDX2 in trophectoderm (TE) cells has been extensively studied, yet the results are contradictory and species specific. Here, CDX2 expression and function were explored in early porcine embryos. Notably, siRNA-mediated gene knockdown and lentivirus-mediated TE-specific gene regulation demonstrated that CDX2 is essential for the maintenance of blastocyst integrity by regulating the BMP4-mediated blastocyst niche and classical protein kinase C (PKC)-mediated TE polarity in mammalian embryos. Mechanistically, *CDX2*-depleted porcine embryos stalled at the blastocyst stage and exhibited apoptosis and inactive cell proliferation possibly resulting from BMP4 downregulation. Moreover, TE cells in *CDX2*-depleted blastocysts displayed defective F-actin apical organization associated with downregulation of PKCα. Collectively, these results provide further insight into the functional diversity of CDX2 in early mammalian embryos.

Introduction

After several cleavage divisions, mammalian zygotes develop into blastocysts comprised of two distinct cell groups: the trophectoderm (TE) and inner cell mass (ICM). The TE is a single layer of polarized epithelial cells that forms the outer wall of the blastocyst and eventually develops into fetal placenta, whereas the ICM consists of pluripotent cells and eventually develops into the embryo proper. As the earliest-born epithelial cells of mammalian embryos, the TE displays tissue characteristics typical of adult epithelia, including concerted action of cell adhesion molecules, intercellular junctions, and an extensive system of intermediate filaments that ensure epithelial integrity and polarized cytoplasmic organization (Fleming et al., 1992; Wiley, 1988). In turn, TE integrity is essential for blastocyst expansion, embryonic patterning, nutrition, and implantation.

In mice, TE identity is maintained by a gene regulatory network (GRN) orchestrated by the transcription factor, caudal-related homeobox protein 2 (Cdx2) (Johnson, 2009). Cdx2 is first detected in some nuclei of the 8- to 16-cell stage mouse embryo and later expands to all blastocystic TE cells (Strumpf et al. 2005; Ralston and Rossant 2008). Cdx2 is one of the earliest transcription factors exhibiting differential expression on outside and inside blastomeres. Prior to the blastocyst stage, Cdx2 becomes spatially restricted to the outer blastomeres immediately before the downregulation of Oct4, Nanog, and Sox2 (Cockburn and Rossant, 2010). Overexpression of *Cdx2* alone was sufficient to commandeer the whole TE GRN and override mouse ES cell pluripotency to induce morphologically and functionally normal trophoblast stem cells (Niwa et al., 2005; Strumpf et al., 2005). *Cdx2*$^{-/-}$ mouse embryos lose TE epithelial integrity and die around the time of implantation (Strumpf et al., 2005), and exogenous *Cdx2* titration in early blastomeres changed their developmental frequency towards TE and ICM via altered cell

polarity (Jedrusik et al., 2008). Collectively, these data suggest that *Cdx2* expression before blastocyst formation plays a pivotal role in TE identity and function in mice.

However, reports on Cdx2 function prior to blastocyst formation are contradictory. Several studies have shown that Cdx2 is not required for mouse cleavage stage development or the apical polarization and cell viability of mouse TE cells (Blij et al., 2012; Ralston and Rossant, 2008; Strumpf et al., 2005; Wu et al., 2010). These studies demonstrated that mouse embryos depleted of *Cdx2* by either gene knockout or RNA interference were able to develop to normal blastocysts in terms of overall cell number, ICM:TE ratio, and TE apical polarity, despite abnormal cell junctions. Furthermore, *Cdx2*-deficient blastomeres contribute to the TE in chimeric embryos at a normal frequency (Ralston and Rossant, 2008). Despite using the same gene knockout and RNA interference approaches, these results are directly contradictory to those reported in other studies, which showed that *Cdx2* depletion compromised cell polarity, and induced developmental arrest before blastocyst stage and significantly reduced blastocyst rate (Jedrusik et al., 2010; Jedrusik et al., 2015). One plausible explanation for this discrepancy could be the different genetic backgrounds among strains. Nevertheless, given the contradictions and ambiguities, the molecular mechanisms associated with Cdx2 function in mouse embryos remain elusive.

CDX2 is also expressed during early embryonic development of other mammals; however, unlike mouse, CDX2 protein is detectable after blastocyst formation in humans (Niakan and Eggan, 2013) and at morula stage in monkeys (Sritanaudomchai et al., 2009). In porcine and bovine, CDX2 is specifically expressed in blastocyst TE cells (Kuijk et al., 2008). Functional analysis of CDX2 in preimplantation embryos using RNAi found that monkey blastocysts failed to hatch (Sritanaudomchai et al. 2009), similar to the mouse, whereas bovine blastocysts hatched normally (Berg et al., 2011). Taken together, these

results indicate that although CDX2 is important for early embryonic development, it exhibits functional diversity among species. As such, it is necessary to study *Cdx2* in multiple species to fully elucidate its function, and these studies will undoubtedly shed light on the molecular regulation of preimplantation development across mammalian species.

In the present study, porcine CDX2 expression was assessed at both mRNA and protein levels in successive stages of preimplantation embryos. In addition, the CDX2 function in porcine embryonic development was systematically explored using siRNA-mediated gene knockdown and lentivirus-mediated TE specific gene regulation.

Results

CDX2 spatiotemporal expression pattern in early-stage porcine embryos

To date, CDX2 expression has only been shown in porcine blastocysts. To gain better insight into the role of CDX2 in early embryonic development, the spatial and temporal dynamics of CDX2 were assessed in early porcine embryos. CDX2 was detected in a subset of TE nuclei in cavitated D5 blastocysts (~20 cells), and all TE cells in expanded D6.5 and hatched D7.5 blastocysts (Fig. 1A, green). No CDX2 signal was observed in the nuclei of cleavage-stage embryos and ICM. Interestingly, OCT4 (Fig. 1A, red) was present in all cells of the embryos, even in D7.5 hatched blastocysts. In vivo CDX2 and OCT4 staining in porcine embryos at these stages were identical to in vitro counterparts (Fig. S1A,B vs. Fig. 1A). Quantitative real-time PCR (qPCR) results indicated that *CDX2* mRNA expression was remarkably increased at the 16-cell stage just before blastocyst formation, but *OCT4* mRNA was steadily expressed during all developmental stages (Fig. 1B). Consistent with the previous RNA sequencing data (Cao et al.,

2014), RT-PCR results confirmed the absence of two other CDX family members, *CDX1* and *CDX4* (3 technical replicates, Fig. S1C). Moreover, western blot (WB) analysis revealed that MII stage oocytes expressed CDX2, but only ~1/400 of that present in D6.5 blastocysts (Fig. 1C). RNA-FISH was performed to further confirm the *CDX2* mRNA expression in early porcine embryos, which clearly showed perinuclear localization (Fig. 1D). The high fluorescence intensity of RNA-FISH was also seen at the 16–cell stage, consistent with our qPCR results (Fig. 1B).

CDX2 knockdown affects total cell number and hatching process in blastocysts without affecting preceding embryonic development

To address CDX2 function in early porcine embryonic development, modified Stealth siRNA against *CDX2* mRNA (Fig. S1D) was injected into porcine zygotes and cultured in vitro for 7 days. Stealth siRNA effectively decreased target gene expression for 3-4 days, during which time mouse embryos develop from zygotes to blastocysts (Wu et al., 2010). Porcine embryos require ~7 days to developing from zygotes to blastocysts in vitro. As such, *CDX2* expression was evaluated by qPCR at different developmental stages after zygotic siRNA injection to monitor the efficacy of injected siRNA. Embryos injected with a scrambled siRNA duplex was used as the control group (siControl embryos), and we set *CDX2* expression of siControl embryos as 100%. As expected, *CDX2* expression was effectively downregulated at least 80% in siCDX2 embryos at D7 and earlier (Fig. 2A). The effective *CDX2* knockdown was also verified by RNA-FISH at the 4-cell and blastocyst stages (Fig. 2B), and by the immunofluorescence (IF) assay in blastocysts (Fig. 2C).

The cleavage rate and D7.5 blastocyst rate were consistent between siCDX2 and siControl embryos; however hatching rate was significantly lower in D7.5 siCDX2 blastocysts compared with the siControl group (0% [0/47] with siCDX2 *vs.* 32% [16/50] with siControl) (Fig. 2D, and Fig. S1G, S1H). In addition, the cell number was significantly lower in D7.5 siCDX2 blastocysts (Fig. 2E), which were smaller in size compared with the siControl group (Fig. 2F). Cytokeratin 8 (CK8) is a TE-specific intermediate filament and serves as a marker of epithelization. Notably, positive CK8 IF signals were observed in the TE of siCDX2 blastocysts, indicative of normal epithelization (Fig. 2G), while the comparable cell numbers between siCDX2 and siControl blastocysts showed that cell proliferation was compromised after blastocyst formation in siCDX2 embryos (Fig. 2E). These results implied that *CDX2* knockdown affect total cell number and the hatching process in blastocysts independent of prior embryonic development**.**

CDX2 is dispensable in blastomere polarization and junction formation prior to the blastocyst stage

Polarization and adherens junctions appear by the 8-cell stage in both mouse (Eckert and Fleming, 2008; Watson, 1992) and porcine (Reima et al., 1993) embryos, but the role of Cdx2 in these events is still under debate. Thus, we investigated *CDX2* function in blastomere polarization given that its mRNA expression observed during cleavage (Fig. 1B; and Fig. S1C). F-actin has been widely used as mouse blastomere polarization marker (Johnson, 2009; Stephenson et al., 2010); therefore, we assessed the effect of *CDX2* knockdown on 8-cell porcine embryo polarization by F-actin staining (Fig. 3A). These results showed that F-actin underwent normal apical polarization at the 8-cell stage in both siCDX2 and siControl embryos. Moreover, E-cadherin (*CDH1*) staining demonstrated that adherens junction assembly was also intact in 8-cell siCDX2 embryos (Fig. 3B). To confirm these findings, the expression of *CDH1* and other

genes associated with polarization (*PAR1*; *PAR3*), cell junctions and compaction (*CTNNB1*, encodes beta-catenin), and cavitation (*ATP1B1*, encodes a Na^+/K^+-ATPase subunit) was examined by qPCR, which showed equivalent expression in 8-cell siCDX2 and siControl embryos ($p>0.05$; Fig. 3C). Collectively, these results suggest that CDX2 is not required to establish cell polarity and junctions prior to the blastocyst formation.

CDX2 maintains TE cell polarity by regulating PKCα (*PRKCA*) expression

CDX2 depletion did not affect the initial formation of polarity and junctions; however, whether *CDX2* depletion affects later blastocyst stages has not been determined. As such, TE apical polarity was examined by F-actin immunostaining and scanning electron microscopy (SEM). Our result showed that F-actin localized apically on siControl blastocysts, but was more evenly distributed in cytoplasm of siCDX2 blastocysts (Fig. 4A). Given that apical F-actin is crucial to establish microvilli, SEM also showed hindered apical microvilli development on TE cells of siCDX2 embryos as compared to siControl counterparts (Fig. 4B). Due to the important role of F-actin in stress fibers (Tojkander et al., 2012), improper F-actin organization might be a potential reason for the hatching failure of siCDX2 blastocysts. Moreover, SEM images clearly showed that the lack of apical microvilli in siCDX2 blastocysts also influenced formation of the superficial ridge structure between cell-cell contact, which is generally composed of microvilli from two adjacent epithelial cells (Gorelik et al., 2003). To determine the key factors mediating the deficient TE polarization and apical micovilli formation in siCDX2 blastocysts, qPCR was performed to analyze genes involved in polarization and micovilli, such as *ACTB*, *EZRIN*, *ARP2*, *CAPZA1* and *PRKCA*. The results showed that *CDX2* depletion did not disturb the *ACTB*, *EZRIN*, *ARP2*, or *CAPZA1* mRNA expression, whereas *PRKCA* was significantly decreased ($P<0.05$) (Fig. 4C).

PRKCA is an important signal transducer that participates in cytoskeleton organization and function (Hong et al., 2011; Ng et al., 2001). As such, *PRKCA* expression was analyzed by qPCR during early porcine embryo development to determine whether its suppression was responsible for the abnormal apical polarity observed in siCDX2 blastocysts. Interestingly, *PRKCA* was maternally expressed in MII oocytes (Fig. 4D), which might be related to its roles in oocyte meiotic maturation and fertilization (Capo-Chichi et al., 2005; Fan et al., 2002). Thereafter, *PRKCA* expression decreased and remained at a low level until significantly increasing during morula-blastocyst transition (Fig. 4D), which corresponds to the period of CDX2 accumulation in the TE. To evaluate whether *PRKCA* expression is directly regulated by CDX2, we analyzed its expression by qPCR 36h after TE-specific, lentivirus-mediated *CDX2*-overexpression or knockdown in D5 blastocysts (Fig. S2A, B). Notably, *CDX2*-knockdown (CDX-miR) embryos showed significantly lower *PRKCA* expression, whereas those with TE-specific red fluorescence protein tagged *CDX2* (CDX-RED) showed a marked increase when compared with controls infected with lentivirus harboring negative control miRNA (Con-miR) or nuclear-localized red fluorescence protein (NLS-RED), or uninfected, intact embryos. After a positive correlation between *CDX2* and *PRKCA* expression was found, the effect of *PRKCA* on TE polarity was examined by siRNA knockdown in porcine embryos. These results demonstrated that *PRKCA* disruption produced the same partial phenotypes as *CDX2* knockdown, including the failure to hatch (Fig. 4F, G), decreased blastocyst cell number ($p<0.05$, Fig. 4H), and loss of TE apical polarity (Fig. 4I).

Previous studies indicated that phosphorylated EZRIN (p-EZRIN) acts as a bridge between F-actin and plasma membrane proteins during apical polarization and that PKCα directly phosphorylates EZRIN (Baiocchi et al., 2008; Hong et al., 2011; Ng et al., 2001; Ren et al., 2009). Thus, EZRIN, p-EZRIN, CDX2,

and PKCα levels were analyzed by WB in siCDX2 and siPKCα blastocysts. As expected, p-EZRIN was significantly lower in siCDX2 and siPKCα blastocysts when compared with siControl blastocysts (Fig. 4J); however, total EZRIN protein levels did not change. Moreover, *CDX2* depletion reduced PKCα expression, but not the opposite (Fig. 4J), indicating that PKCα is downstream of CDX2. These results were confirmed by p-EZRIN immunostaining, which showed that both siCDX2 and siPKCα blastocysts lacked apically localized p-EZRIN (Fig. 4K). Collectively, these results strongly suggest that CDX2 is essential for maintaining cell polarity in the TE by inducing PKCα expression.

Since epithelial cell junctions and apical polarity are mutually dependent (Shin et al., 2006; Tepass, 2012), TE cell junctions were examined in siCDX2 blastocysts. Tight junctions are formed as a rather late molecular event that relies on both cell polarization and intact adherens junctions (Eckert and Fleming, 2008; Sheth et al., 2006). ZO-1 immunostaining at different developmental stages confirmed that tight junctions were established at the morula stage in porcine embryos (Fig. S3A). Moreover, we found that *ZO-1* mRNA expression (Fig. 4L) and protein assembly was normal in siCDX2 embryos at D6.5 (Fig. S3B), but mRNA was significantly upregulated at D7.5 (Fig. 4L, $p<0.05$). Additionally, although *CDH1* mRNA was comparable in siCDX2 and siControl embryos (Fig. 4L), E-cadherin localization was more diffuse at the TE cell border in siCDX2 blastocysts (Fig. 4M), implying that adherens junctions in porcine TE is disrupted in the absence of *CDX2* expression. Therefore, disrupted lateral junction formation, which is important for cavity sealing, may be another factor aggravates the hatching failure of siCDX2 blastocysts, and has been mentioned in mice (Strumpf et al., 2005; Wu et al., 2010).

CDX2 is important to blastocyst cell viability and proliferation possibly by maintaining the BMP4 mediated blastocyst niche

To gain further insight into the decreased cell number in *CDX2* deficient blastocysts, apoptosis was assessed via cleaved caspase 3 (Fig. 5A) and terminal deoxynucleotidyl transferase dUTP nick end labeling (TUNEL) staining (Fig. 5B). Consistent with our observation, quantification of TUNEL analysis indicated a high-rate apoptosis in siCDX2 blastocysts (Fig.5C).

Subsequently, we examined the expression of select genes related to blastocyst development to evaluate the further development of siCDX2 embryos (Fig 5D, E). The results showed that genes responsible for TE development, *EOMES*, *ELF5*, and *GCM1* were down-regulated in D6.5 siCDX2 blastocysts; *CDH3* (placental cadherin), and *HAND1* (a gene important to placental development) were down-regulated in D7.5 siCDX2 blastocysts; and *FGFR2* (a signaling receptor important for elongation) was down-regulated in both D6.5 and D7.5 siCDX2 blastocysts (Fig. 5D). However key transcription factors for ICM development, *SOX2* and *NANOG*, were both significantly up-regulated in siCDX2 blastocysts, although *OCT4* was not (Fig. 5E). IF staining indicated that SOX2 expression was retained in TE of siCDX2 blastocysts, whereas it was repressed in that of siControl blastocysts (Fig. 5F). Moreover, qPCR analysis of genes related to paracrine pro-proliferative factors (Fig. 5G) showed that *BMP4* expression was slightly up-regulated ($p>0.05$) in D6.5 siCDX2 blastocysts when compared to siControl embryos, but subsequently diminished ($p<0.05$) at D7.5 only in siCDX2 blastocysts. The expression of both *LIF* and its receptor *LIFR* were also substantially increased in D7.5 siCDX2 blastocysts, while *bFGF (FGF2)* expression was comparable between siCDX2 and siControl embryos. However, expression of

FGF4 was decreased, while that of its receptor, *FGFR1*, was increased in D6.5 siCDX2 blastocysts. In mouse blastocysts, Cdx2 transcriptionally promotes *Bmp4* expression in TE cells, which is subsequently secreted and binds the ICM to promote proliferation and *Fgf4* expression (Murohashi et al., 2010). In the current study, *BMP4* expression was increased at the blastocyst stage during normal porcine development, consistent with *CDX2* upregulation (Fig. S4B), however, both *BMP4* and *FGF4* were down-regulated in siCDX2 blastocysts. In addition, we found that the BMP4 receptor, BMPR2, was expressed specifically in the porcine ICM (Fig. 6A). Together with previous reports of FGF4 expression specifically in the porcine ICM (Fujii et al., 2013), we speculated that CDX2-BMP4-FGF4 circuit observed in mice (Murohashi et al., 2010) might also be present in porcine embryos.

Based on this rationale, the effect of CDX2-BMP4 regulation on cell proliferation was examined in blastocysts infected with TE-specific CDX-miR or CDX-RED lentivirus. Notably, *BMP4* expression was significantly higher in *CDX2*-overexpressing blastocysts at D6.5 than that in knockdown or control embryos (Fig. 6B). However, *CDX2*-overexpressing blastocysts severely degenerated at D7.5, most likely resulting from a harmful CDX2 overdose (Bou et al., 2016) (Fig. S2B). In TE-specific *CDX2*-knockdown embryos, *BMP4* failed to increase at D7.5 and was significantly lower than observed in the three control groups (Fig. 6B). Meanwhile, the average ICM number in D7.5 blastocysts was significantly increased ($p<0.05$) after TE-specific *CDX2* over-expression, although the average total and TE number were decreased, most likely because of TE degeneration (Fig. 6C). Furthermore, both total cell number and TE cell number were significantly reduced compared to three control groups in TE-specific *CDX2* knockdown embryos (Fig. 6C).

To confirm the functional significance of BMP4 on porcine blastocyst proliferation, cell numbers were determined in D7.5 balstocysts treated with BMP4 or the BMP4 antagonist, Noggin, starting on D5. As expected, BMP4 supplementation significantly increased cell numbers in both siControl and siCDX2 blastocysts (Fig. 6D; Fig. S4A), whereas Noggin supplementation inhibited cell proliferation specifically in siControl blastocysts (Fig. 6E), indicating that *BMP4* is essential for porcine blastocyst proliferation.

Collectively these results support our conjecture and suggest that CDX2 is important to blastocyst cell viability and proliferation possibly by maintaining the BMP4-mediated blastocyst niche in pigs.

CDX2 over-expressing blastomeres preferentially contribute to TE development

Mouse studies have shown that Cdx2 is heterogeneously expressed in early blastomeres at cleavage (Dietrich and Hiiragi, 2007) and believed to contribute to lineage specification (Niwa et al., 2005). However, data from several studies show contradictory effects following exogenous *Cdx2* expression regulation in early blastomeres (Jedrusik et al., 2008; Ralston and Rossant, 2008). Thus, we examined whether *CDX2* regulation in porcine blastomeres during cleavage influences their developmental fate. For this, *CDX2* siRNA or mRNA, along with episomal plasmid expressing EGFP (pS/MAR-EGFP), were injected into one blastomere of 4-cell porcine embryo and the distribution of EGFP positive cells was traced in blastocysts (Fig. 7A). Result showed that the blastocysts segregated into three groups: “ICM only” (all EGFP-positive cells contributed to the ICM), “TE only” (all EGFP-positive cells contributed to TE), or “ICM&TE” (positive cells found in both ICM and TE) (Fig. 7B). Interestingly, the proportion of “TE only” embryos was significantly increased in *CDX2* over-expressing group (Fig. 7C; $p<0.05$), whereas no

significant difference was found between the *CDX2* knockdown and control groups. Thus, these data suggest that CDX2 plays an important role in the GRN controlling the molecular features of TE in porcine embryos, but was not enough to determine TE fate.

Discussion

Genes are known to show species-specific expressional patterns or functions in mammal. For example, *Cdx2* expression in early mouse embryos resembles neither the human (Niakan and Eggan, 2013) nor the monkey (Sritanaudomchai et al., 2009). Cdx2 is a major regulator of initial lineage segregation and trophoblast stem cell properties. The current study indicated that the CDX2 expression pattern in porcine embryos is relatively similar to that of humans, in which CDX2 upregulated in TE cells after blastocyst formation (Niakan and Eggan, 2013). As such, exploring CDX2 function in porcine embryos might enhance knowledge of molecular regulation in embryology in general and shed light on the function of CDX2 in human development.

The spatiotemporal expression of CDX2 in porcine embryo differs from that of mouse embryo (Dietrich and Hiiragi, 2007) (Fig. 7D). In mice, CDX2 protein is first detected in some blastomeres of 8-cell stage embryos and becomes restricted to the TE by E3.5. In contrast, porcine CDX2 protein initially observed in some TE cells right after cavitation at E5 and remains exclusively in TE thereafter. Interestingly, the time-point for porcine CDX2 protein expression is very similar to that in bovine (Goissis and Cibelli, 2014; Madeja et al., 2013) and human (Niakan and Eggan, 2013) embryos, in which CDX2 protein becomes detectable after blastocyst formation. Similarly, prolonged Oct4 expression in TE is also observed in human (Cauffman et al., 2005) and bovine (van Eijk et al., 1999) embryos. Since CDX2

accumulation is primed by Hippo signaling in response to cell contact and positional information in mice (Hirate and Sasaki, 2014; Nishioka et al., 2009), it would be interesting to explore whether this signaling pathway exists in porcine embryos, as this knowledge would expand our mechanistic understanding of the various *Cdx2* expression patterns observed in mammalian embryos.

The current data on Cdx2 function in mouse embryos before blastocyst formation is contradictory (Bruce, 2011; Wu and Scholer, 2011). Our results derived from *CDX2* knockdown porcine embryos indicate that CDX2 is not essential before blastocyst formation, since the siCDX2 blastocyst rate was no different from that of the control. This result is consistent with several studies in mice, which showed that *Cdx2* mutant (Strumpf et al., 2005) or knockdown (Wu et al., 2010) embryos developed normally to blastocyst stage; however, others have found that *Cdx2* depletion induced developmental arrest before blastocyst formation (Jedrusik et al., 2010; Jedrusik et al., 2015). Different time-points for Cdx2/CDX2 accumulation may account for different *Cdx2/CDX2*-depleted embryo phenotypes in mouse and pig. Therefore, the results from porcine studies may be more pertinent to our understanding of CDX2 function in embryonic development in large animals, including bovines and primates, which also share same time-points for CDX2 accumulation (Goissis and Cibelli, 2014; Madeja et al., 2013; Niakan and Eggan, 2013). However, more studies in strains are needed to clarify the functional significance of Cdx2 in mouse cleavage stage embryos (Wu and Scholer, 2011).

The effect of Cdx2 on mouse TE fate commitment is still a matter of debate. Results from a study by Jedrusik et al. (Jedrusik et al., 2008) indicated that Cdx2 is a key factor in TE fate commitment, as increased *Cdx2* expression in individual blastomeres promoted differentiation towards the TE lineage, and hindered that of ICM. In contrast, Ralston and Rossant (2008) indicated that Cdx2 functions downstream

of lineage allocation since *Cdx2*-depleted blastomeres do not preferentially contribute to ICM. Our study found that cell polarization and junctions in siCDX2 porcine embryos before blastocyst stage were similar with control. Although *CDX2*-overexpressing blastomeres from 4-cell stage embryos contributed to the TE at a higher rate, *CDX2* down-regulated blastomeres did not similarly contribute to the ICM. Consistent with our results, a bovine study (Goissis and Cibelli, 2014) indicated that *CDX2* depletion does not affect the blastocyst rate and TE, ICM or total cell number. Interestingly, although CDX2 is first detectable at the morula-stage monkey embryos, CDX2 knockdown did not affect blastocyst formation (Sritanaudomchai et al., 2009). Collectively, these results suggest that CDX2 is not involved in TE fate decision in large animal embryos.

Data regarding the role of Cdx2 on TE cells and further development of blastocysts is similar among different studies and different species. In mice, both *Cdx2*-knockout and knockdown blastocysts exhibit hatching failure, decreased cell number, abnormal TE cell junctions/polarity, and disturbed TE GRN (Blij et al., 2012; Jedrusik et al., 2010; Jedrusik et al., 2015; Nishioka et al., 2008; Ralston and Rossant, 2008; Strumpf et al., 2005; Wu et al., 2010). In primates (Sritanaudomchai et al., 2009) and cattle (Goissis and Cibelli, 2014; Madeja et al., 2013), *CDX2* knockdown resulted in hatching failure and deficient cell proliferation in blastocysts. Consistently, our study also showed that *CDX2* knockdown compromised TE cell polarization and junctions. Furthermore, our results indicated that PKCα is a key intermediary for the effect of CDX2 on TE cell polarity.

A Cdx2-Bmp4-Fgf4 functional circuit has been shown in mouse embryos (Murohashi et al., 2010). Similarly, our study determined that BMP4 promoted blastocyst cell proliferation and was regulated by CDX2 in the TE of porcine blastocysts. This suggests that BMP4 down-regulation in siCDX2 porcine

embryos is partially responsible for the deceased cell number, along with the increasing rate of apoptosis. Thus, it is also reasonable to conclude that hatching failure phenotype seen in siCDX2 porcine embryos could result from defects in cell proliferation, as well as TE cell junction/ polarity. Despite the discrepancy in CDX2 function prior to blastocyst formation between species, its participation in TE maintenance is clearly necessary for blastocyst development among various mammals.

It is noteworthy that Cdx2 plays species-specific roles in regulating trophoblast-related gene expression. Reports from mouse trophoblast stem cell studies showed that Cdx2, Eomes, and Elf5 form a positive feed-back loop that maintains lineage fate (Ng et al., 2008). However, according to the previous study (Valdez Magana et al., 2014), this loop may not exist in the porcine trophoblast lineage, since EOMES and ELF5 are only highly expressed in tubular-stage porcine embryos, when *CDX2* expression in TE cells has already down-regulated, and ELF5 does not co-express with CDX2 in the porcine TE. Thus, it is assumed that, CDX2 does not transcriptionally up-regulate *EOMES/ELF5* expression in porcine TE, but more likely that CDX2 and EOMES/ELF5 control of TE GRN at the early and later stages, respectively. Therefore, higher *EOMES* and *ELF5* levels in siCdx2 D7.5 porcine embryos might occur due to a compensative mechanism following *CDX2* downregulation.

Along with Cdx2 studies in other mammalian embryos, the current study of porcine embryos highlights the importance of Cdx2 in early mammalian development. In Fig. 7D, we compare preimplantation embryonic development between mouse and pig, in vitro and in vivo and include key developmental events such as ZGA, compaction, cavitation and implantation. In addition, to clarify, the key results of this study are summarized in Fig. 7E. Comparisons of embryonic development among multiple mammalian species will not only improve overall knowledge of mammalian embryonic

development, but also provide clues to find more suitable animal models for human embryonic development. Collectively, our findings provide nascent ideas on CDX2 function in human embryonic development, especially with regard to TE development, due to the similarities in CDX2 spatiotemporal expression patterns between pig and human embryos.

Materials and methods

In vitro embryo production and culture

All animal procedures conformed to the guidelines and regulatory standards of the Animal Care and Use Committee of Northeast Agricultural University. Porcine oocytes were matured in vitro, as previously described (Liu et al., 2008). To generate in vitro fertilization embryos, denuded oocytes were washed and held in modified Tris-buffered medium prior to fertilization with standard procedures (Abeydeera and Day, 1997). Presumptive zygotes were then cultured in PZM-3 medium (Yoshioka et al., 2002) for 7 days at 39°C with a 5% CO2 atmosphere. Cleavage rates were evaluated at D2 by microscopy, whereas blastocyst and hatching rates were assessed at D7.5. Cell numbers at D5, 6.5, and 7.5 were qualified by DAPI nuclear staining.

In vivo embryo collection

In vivo embryos were collected from Yorkshire-Danish Landrace sows from days 1- to 6 post-insemination. The sows were mated twice within 24 h after detection of estrus, at an interval of 12 h. The last mating time was taken to be day 0 (D0) of conception. Reproductive organs collected from the sows were transported to the laboratory in warm saline (37 °C) for a maximum period of 1 h. Embryos were rinsed twice using 50 mL phosphate-buffered saline (PBS) supplemented with 5% fetal bovine serum (FBS). All procedures were approved by the Animal Ethics Committee of the Northeast Agriculture University, Harbin, China.

Whole embryonic and single blastomeric *CDX2* regulation via RNA injection

Stealth siRNA against porcine *CDX2* designed with BLOCK-iT RNAi Designer was injected into zygotes or one blastomere of a 4-cell stage porcine embryo. The highest effective duplex selected from 3 Stealth

siRNA was as follows:

*siCDX2*sense: 5'CGAAAGACAAAUACCGAGUCGUGUA3';

siCDX2 antisense: 5'UACACGACUCGGUAUUUGUCUUUCG3'.

CDX2 siRNA efficiency and specificity demonstrated with porcine intestinal epithelial cells (Fig. S1E). At the same time, a scrambled siRNA duplex with the same nucleotide composition but no specific target was used as the control. The sequence of control siRNA was as follows:

siControl sense:5'CGAACAGAUAAAGCCGCUGUAAGUA3';

siControl antisense: 5'UACUUACAGCGGCUUUAUCUGUUCG3'.

CDX2 was overexpressed in one blastomere of 4-cell stage porcine embryo by mRNA injection. The *CDX2* full-length ORF was cloned from cDNA of porcine blastocyst and inserted into pMACS KkHA(N) plasmid (Miltenyi Biotec) and used for in vitro transcription (RIBOMAX Large Scale RNA Production System T7 kit, Promega). The PCR primers used were as follows:

CDX2F: 5'ATGTACGTGAGCTACCTCCTGGACAAGGAC3';

CDX2R: 5'CTGGGTGACGGTGGGGTTTAACACGC3'.

Microinjection of si/mRNA was performed using Eppendorf FemtoJet microinjector and Narishige NT-88NE micromanipulators. A glass capillary femtotipII (Eppendorf) was loaded with 5 μL RNA (20 nM siRNA, 50 ng/μL mRNA) using a microloader (Eppendorf) and about 30 pL of solution was injected into the zygote or blastomere cytoplasm. To trace the fate of injected single blastomeres, 20 ng/μL episomal plasmid pS/MAR-EGFP was co-injected with si/mRNA, or alone as control. Microinjection efficiency in this study was near 100% as proven by injecting *GFP* mRNA under the same conditions (Fig. S1F).

TE-specific *CDX2* regulation via lentivirus infection of D5 blastocysts

To achieve TE specific *CDX2* regulation, the zona pellucida was removed from D5 early cavitated embryos with pronase and then washed. Each of 15 blastocysts was then infected in 30 μL equilibrated PZM3 containing 5×10^6 cfu lentivirus in mineral oil and incubated at 39°C with 5% CO_2 for 3 h. Infected embryos were then washed and cultured in 500 μL fresh PZM3. Total numbers of ICM and TE cells were calculated based on nuclear, CDX2/OCT4, and fluorescent signals (Fig.S2C). The procedures for obtaining different lentiviruses with FUW backbone were described previously (Zhi et al., 2014).

siRNA mediated *PRKCA* and *ZO-1* knockdown

Stealth siRNAs against porcine *PRKCA* and *ZO-1* were designed in BLOCK-iT RNAi Designer. Because PKCα functions before the first-cleavage (Capo-Chichi et al., 2005; Fan et al., 2002), *PRKCA* knockdown was accomplished by injecting siRNA into all blastomeres of 2-cell embryos. *ZO-1* siRNA was injected into zygotes for knockdown. Stealth siRNA for *PRKCA* and *ZO-1* are:

siPRKCA sense: 5'UGGUUCACAAGAGGUGCCAUGAGUU3';

siPRKCA antisense: 5'AACUCAUGGCACCUCUUGUGAACCA3'; and

siZO1 sense: 5'GCGCUACAAGUGAUGACCUUGAUUU3';

si*ZO1* antisense: 5'AAAUCAAGGUCAUCACUUGUAGCGC3'.

Negative control siRNA (Cat#12935300, Invitrogen) was used as control siRNA for the above knockdown experiments.

RNA-FISH

Embryos were fixed with 4% PFA, overnight at 4°C, and stored in methanol at −20°C. *In situ* hybridization was performed as previously described (Chazaud et al., 2006) with slight modifications. RNA probes for porcine *CDX2* were generated by in vitro transcription of 936-bp full length cDNA cloned in pSPT18 plasmid. The sense and antisense probes were synthesized in vitro under control of the T7 and SP2 promoters respectively and labeled with digoxigenin-UTP using a DIG RNA labeling kit (SP6/T7) (Roche). The slide was sealed with ProLong Gold antifade reagent (Invitrogen) and visualized on a Leica TCS SP2 confocal microscope with a 40× oil immersion objective.

RNA isolation, cDNA synthesis and qPCR analysis

For real-time analysis of gene expression, 100 oocytes and embryos were harvested in 10 µL RLT buffer and RNA was extracted with PureLink Micro-to-Midi total RNA purification kit with Dnase I treatment (Invitrogen). The cDNA synthesis was performed using High capacity cDNA reverse transcription kits (ABI).

The cDNA (~8 oocytes/embryos per reaction) was used in 50 µL real-time reactions (SYBR Premix Ex Taq for Perfect Real Time, Takara) using oligonucleotide primers (Table S1). All transcripts levels were normalized against 18s rRNA for oocyte and embryo samples (Kuijk et al., 2007). For porcine intestinal epithelial cells, the ribosomal protein L4 RNA (Nygard et al., 2007) was used as reference gene. qPCR was performed with the ABI 7500 real-time PCR system. Three to six biological and three technical replicates were performed. The $2^{-\Delta\Delta}$Ct method was used for relative quantification analysis. To determine knockdown efficacy, embryos injected with a scrambled siRNA duplex were used as controls (siControl embryos), and we set *CDX2* expression of siControl embryos at 100%.

WB and IF assay

WB and IF experiments in porcine embryos were conducted as previously described (Bou et al., 2016) with the antibodies described in Table S2.

Scanning electron microscopy (SEM)

After removing the zona pellucida, embryos were processed as previously described (Xia et al., 2011) and imaged with a S-3400N (Hitachi) microscope.

TUNEL assay

Apoptosis was determined by TUNEL technique. DNA strand breaks were directly labeled with red fluorescent using tetra-methyl-rhodamine-dUTP (In situ Cell Death detection kit, TMR red, Roche), as described previously (Hao et al., 2004).

Statistical analysis

Each experiment was repeated at least three times; and representative images are shown in figures. All values are reported as the mean±SD Statistical calculations were performed in GraphPad Prism 6 (GraphPad software Inc.). To compare the gene expression levels, embryonic development rate, we used unpaired two-tailed Student's t-tests (parametric) or unpaired, two-tailed Mann–Whitney U-tests (non-parametric) when analyzing two groups. The one-way ANOVA with Turkey's post hoc testing (parametric) or Kruskal–Wallis test with Dunn's correction for multiple comparisons (non-parametric) was used to analyze multiple groups, mainly when comparing cell numbers. The F-test, Browne–Forsythe test or Bartlett's test was used to determine the distributional assumption (normality and homogeneity of variance) of the data. Non-parametric tests were used when data did not fit a normal distribution. Significant differences were defined as $P<0.05$. Differences are shown with "*", or different letters "a, b, c."

Acknowledgements

We thank Lin Cui and Xuedong Wang (Northeast Agricultural University) for SEM and LetPub (www.letpub.com) for linguistic assistance.

Competing interests

The authors declare no competing financial interests.

Author contributions

G.B. and Z.L. designed experiments; All authors except Z.L. performed experiments; G.B. and Z.L. analyzed the data and wrote the manuscript.

Funding

This work was supported by the National Basic Research Program of China [2011CB944202], the National Natural Science Foundation of China [31371457, 31401228] and the Fostering Talents in Basic Science of the National Natural Science Foundation of China [J1210069].

Reference

Abeydeera, L. R. and Day, B. N. (1997). Fertilization and subsequent development in vitro of pig oocytes inseminated in a modified tris-buffered medium with frozen-thawed ejaculated spermatozoa. *Biology of reproduction* **57**, 729-734.

Baiocchi, L., Tisone, G., Russo, M. A., Longhi, C., Palmieri, G., Volpe, A., Almerighi, C., Telesca, C., Carbone, M., Toti, L., et al. (2008). TUDCA prevents cholestasis and canalicular damage induced by ischemia-reperfusion injury in the rat, modulating PKCalpha-ezrin pathway. *Transplant international : official journal of the European Society for Organ Transplantation* **21**, 792-800.

Berg, D. K., Smith, C. S., Pearton, D. J., Wells, D. N., Broadhurst, R., Donnison, M. and Pfeffer, P. L. (2011). Trophectoderm lineage determination in cattle. *Dev Cell* **20**, 244-255.

Blij, S., Frum, T., Akyol, A., Fearon, E. and Ralston, A. (2012). Maternal Cdx2 is dispensable for mouse development. *Development* **139**, 3969-3972.

Bou, G., Liu, S., Guo, J., Zhao, Y., Sun, M., Xue, B., Wang, J., Wei, Y., Kong, Q. and Liu, Z. (2016). Cdx2 represses Oct4 function via inducing its proteasome-dependent degradation in early porcine embryos. *Dev Biol* **410**, 36-44.

Bruce, A. W. (2011). What is the role of maternally provided Cdx2 mRNA in early mouse embryogenesis? *Reprod Biomed Online* **22**, 512-515.

Cao, S., Han, J., Wu, J., Li, Q., Liu, S., Zhang, W., Pei, Y., Ruan, X., Liu, Z., Wang, X., et al. (2014). Specific gene-regulation networks during the pre-implantation development of the pig embryo as revealed by deep sequencing. *BMC Genomics* **15**, 4.

Capo-Chichi, C. D., Rula, M. E., Smedberg, J. L., Vanderveer, L., Parmacek, M. S., Morrisey, E. E., Godwin, A. K. and Xu, X. X. (2005). Perception of differentiation cues by GATA factors in primitive endoderm lineage determination of mouse embryonic stem cells. *Dev Biol* **286**, 574-586.

Cauffman, G., Van de Velde, H., Liebaers, I. and Van Steirteghem, A. (2005). Oct-4 mRNA and protein expression during human preimplantation development. *Mol Hum Reprod* **11**, 173-181.

Chazaud, C., Yamanaka, Y., Pawson, T. and Rossant, J. (2006). Early lineage segregation between epiblast and primitive endoderm in mouse blastocysts through the Grb2-MAPK pathway. *Dev Cell* **10**, 615-624.

Cockburn, K. and Rossant, J. (2010). Making the blastocyst: lessons from the mouse. *J Clin Invest* **120**, 995-1003.

Dietrich, J. E. and Hiiragi, T. (2007). Stochastic patterning in the mouse pre-implantation embryo. *Development* **134**, 4219-4231.

Eckert, J. J. and Fleming, T. P. (2008). Tight junction biogenesis during early development. *Biochim Biophys Acta* **1778**, 717-728.

Fan, H. Y., Tong, C., Li, M. Y., Lian, L., Chen, D. Y., Schatten, H. and Sun, Q. Y. (2002). Translocation of the classic protein kinase C isoforms in porcine oocytes: implications of protein kinase C involvement in the regulation of nuclear activity and cortical granule exocytosis. *Exp Cell Res* **277**, 183-191.

Fleming, T. P., Javed, Q. and Hay, M. (1992). Epithelial differentiation and intercellular junction formation in the mouse early embryo. *Dev Suppl*, 105-112.

Fujii, T., Sakurai, N., Osaki, T., Iwagami, G., Hirayama, H., Minamihashi, A., Hashizume, T. and Sawai, K. (2013). Changes in the expression patterns of the genes involved in the segregation and function of inner cell mass and trophectoderm lineages during porcine preimplantation development. *J Reprod Dev* **59**, 151-158.

Goissis, M. D. and Cibelli, J. B. (2014). Functional characterization of CDX2 during bovine preimplantation development in vitro. *Mol Reprod Dev* **81**, 962-970.

Gorelik, J., Shevchuk, A. I., Frolenkov, G. I., Diakonov, I. A., Lab, M. J., Kros, C. J., Richardson, G. P., Vodyanoy, I., Edwards, C. R., Klenerman, D., et al. (2003). Dynamic assembly of surface structures in living cells. *Proc Natl Acad Sci U S A* **100**, 5819-5822.

Hao, Y., Lai, L., Mao, J., Im, G. S., Bonk, A. and Prather, R. S. (2004). Apoptosis in parthenogenetic preimplantation porcine embryos. *Biol Reprod* **70**, 1644-1649.

Hirate, Y. and Sasaki, H. (2014). The role of angiomotin phosphorylation in the Hippo pathway during preimplantation mouse development. *Tissue barriers* **2**, e28127.

Hong, S. H., Osborne, T., Ren, L., Briggs, J., Mazcko, C., Burkett, S. S. and Khanna, C. (2011). Protein kinase C regulates ezrin-radixin-moesin phosphorylation in canine osteosarcoma cells. *Veterinary and comparative oncology* **9**, 207-218.

Jedrusik, A., Bruce, A. W., Tan, M. H., Leong, D. E., Skamagki, M., Yao, M. and Zernicka-Goetz, M. (2010). Maternally and zygotically provided Cdx2 have novel and critical roles for early development of the mouse embryo. *Dev Biol* **344**, 66-78.

Jedrusik, A., Cox, A., Wicher, K., Glover, D. M. and Zernicka-Goetz, M. (2015). Maternal-zygotic knockout reveals a critical role of Cdx2 in the morula to blastocyst transition. *Dev Biol* **398**, 147-152.

Jedrusik, A., Parfitt, D. E., Guo, G., Skamagki, M., Grabarek, J. B., Johnson, M. H., Robson, P. and Zernicka-Goetz, M. (2008). Role of Cdx2 and cell polarity in cell allocation and specification of trophectoderm and inner cell mass in the mouse embryo. *Genes Dev* **22**, 2692-2706.

Johnson, M. H. (2009). From mouse egg to mouse embryo: polarities, axes, and tissues. *Annu Rev Cell Dev Biol* **25**, 483-512.

Kuijk, E. W., du Puy, L., van Tol, H. T., Haagsman, H. P., Colenbrander, B. and Roelen, B. A. (2007). Validation of reference genes for quantitative RT-PCR studies in porcine oocytes and preimplantation embryos. *BMC Dev Biol* **7**, 58.

Kuijk, E. W., Du Puy, L., Van Tol, H. T., Oei, C. H., Haagsman, H. P., Colenbrander, B. and Roelen, B. A. (2008). Differences in early lineage segregation between mammals. *Dev Dyn* **237**, 918-927.

Liu, Z. H., Song, J., Wang, Z. K., Tian, J. T., Kong, Q. R., Zheng, Z., Yin, Z., Gao, L., Ma, H. K., Sun, S., et al. (2008). Green fluorescent protein (GFP) transgenic pig produced by somatic cell nuclear transfer. *Chin. Sci. Bull.* **53**, 1035-1039.

Madeja, Z. E., Sosnowski, J., Hryniewicz, K., Warzych, E., Pawlak, P., Rozwadowska, N., Plusa, B. and Lechniak, D. (2013). Changes in sub-cellular localisation of trophoblast and inner cell mass specific transcription factors during bovine preimplantation development. *BMC Dev Biol* **13**, 32.

Murohashi, M., Nakamura, T., Tanaka, S., Ichise, T., Yoshida, N., Yamamoto, T., Shibuya, M., Schlessinger, J. and Gotoh, N. (2010). An FGF4-FRS2alpha-Cdx2 axis in trophoblast stem cells induces Bmp4 to regulate proper growth of early mouse embryos. *Stem Cells* **28**, 113-121.

Ng, R. K., Dean, W., Dawson, C., Lucifero, D., Madeja, Z., Reik, W. and Hemberger, M. (2008). Epigenetic restriction of embryonic cell lineage fate by methylation of Elf5. *Nat Cell Biol* **10**, 1280-1290.

Ng, T., Parsons, M., Hughes, W. E., Monypenny, J., Zicha, D., Gautreau, A., Arpin, M., Gschmeissner, S., Verveer, P. J., Bastiaens, P. I., et al. (2001). Ezrin is a downstream effector of trafficking PKC-integrin complexes involved in the control of cell motility. *EMBO J* **20**, 2723-2741.

Niakan, K. K. and Eggan, K. (2013). Analysis of human embryos from zygote to blastocyst reveals distinct gene expression patterns relative to the mouse. *Dev Biol* **375**, 54-64.

Nishioka, N., Inoue, K., Adachi, K., Kiyonari, H., Ota, M., Ralston, A., Yabuta, N., Hirahara, S., Stephenson, R. O., Ogonuki, N., et al. (2009). The Hippo signaling pathway components Lats and Yap pattern Tead4 activity to distinguish mouse trophectoderm from inner cell mass. *Dev Cell* **16**, 398-410.

Nishioka, N., Yamamoto, S., Kiyonari, H., Sato, H., Sawada, A., Ota, M., Nakao, K. and Sasaki, H. (2008). Tead4 is required for specification of trophectoderm in pre-implantation mouse embryos. *Mech Dev* **125**,

270-283.

Niwa, H., Toyooka, Y., Shimosato, D., Strumpf, D., Takahashi, K., Yagi, R. and Rossant, J. (2005). Interaction between Oct3/4 and Cdx2 determines trophectoderm differentiation. *Cell* **123**, 917-929.

Nygard, A. B., Jorgensen, C. B., Cirera, S. and Fredholm, M. (2007). Selection of reference genes for gene expression studies in pig tissues using SYBR green qPCR. *BMC Mol Biol* **8**, 67.

Ralston, A. and Rossant, J. (2008). Cdx2 acts downstream of cell polarization to cell-autonomously promote trophectoderm fate in the early mouse embryo. *Dev Biol* **313**, 614-629.

Reima, I., Lehtonen, E., Virtanen, I. and Flechon, J. E. (1993). The cytoskeleton and associated proteins during cleavage, compaction and blastocyst differentiation in the pig. *Differentiation* **54**, 35-45.

Ren, L., Hong, S. H., Cassavaugh, J., Osborne, T., Chou, A. J., Kim, S. Y., Gorlick, R., Hewitt, S. M. and Khanna, C. (2009). The actin-cytoskeleton linker protein ezrin is regulated during osteosarcoma metastasis by PKC. *Oncogene* **28**, 792-802.

Sheth, B., Eckert, J., Thomas, F. and Fleming, T. (2006). Tight Junctions during Development. In *Tight Junctions*, pp. 164-174: Springer US.

Shin, K., Fogg, V. C. and Margolis, B. (2006). Tight junctions and cell polarity. *Annu Rev Cell Dev Biol* **22**, 207-235.

Sritanaudomchai, H., Sparman, M., Tachibana, M., Clepper, L., Woodward, J., Gokhale, S., Wolf, D., Hennebold, J., Hurlbut, W., Grompe, M., et al. (2009). CDX2 in the formation of the trophectoderm lineage in primate embryos. *Dev Biol* **335**, 179-187.

Stephenson, R. O., Yamanaka, Y. and Rossant, J. (2010). Disorganized epithelial polarity and excess trophectoderm cell fate in preimplantation embryos lacking E-cadherin. *Development* **137**, 3383-3391.

Strumpf, D., Mao, C. A., Yamanaka, Y., Ralston, A., Chawengsaksophak, K., Beck, F. and Rossant, J. (2005). Cdx2 is required for correct cell fate specification and differentiation of trophectoderm in the mouse blastocyst. *Development* **132**, 2093-2102.

Tepass, U. (2012). The apical polarity protein network in Drosophila epithelial cells: regulation of polarity, junctions, morphogenesis, cell growth, and survival. *Annu Rev Cell Dev Biol* **28**, 655-685.

Tojkander, S., Gateva, G. and Lappalainen, P. (2012). Actin stress fibers--assembly, dynamics and biological roles. *J Cell Sci* **125**, 1855-1864.

Valdez Magana, G., Rodriguez, A., Zhang, H., Webb, R. and Alberio, R. (2014). Paracrine effects of

embryo-derived FGF4 and BMP4 during pig trophoblast elongation. *Dev Biol* **387**, 15-27.

van Eijk, M. J., van Rooijen, M. A., Modina, S., Scesi, L., Folkers, G., van Tol, H. T., Bevers, M. M., Fisher, S. R., Lewin, H. A., Rakacolli, D., et al. (1999). Molecular cloning, genetic mapping, and developmental expression of bovine POU5F1. *Biol Reprod* **60**, 1093-1103.

Watson, A. J. (1992). The cell biology of blastocyst development. *Mol Reprod Dev* **33**, 492-504.

Wiley, L. M. (1988). Trophectoderm: the first epithelium to develop in the mammalian embryo. *Scanning Microsc* **2**, 417-426.

Wu, G., Gentile, L., Fuchikami, T., Sutter, J., Psathaki, K., Esteves, T. C., Arauzo-Bravo, M. J., Ortmeier, C., Verberk, G., Abe, K., et al. (2010). Initiation of trophectoderm lineage specification in mouse embryos is independent of Cdx2. *Development* **137**, 4159-4169.

Wu, G. and Scholer, H. R. (2011). Role of mouse maternal Cdx2: what's the debate all about? *Reprod Biomed Online* **22**, 516-518; discussion 519-520.

Xia, P., Liu, Z. and Qin, P. (2011). Fine structures of embryonic discs of in vivo post-hatching porcine blastocysts at the pre-primitive streak stage. *Reprod Domest Anim* **46**, 366-372.

Yoshioka, K., Suzuki, C., Tanaka, A., Anas, I. M. and Iwamura, S. (2002). Birth of piglets derived from porcine zygotes cultured in a chemically defined medium. *Biology of reproduction* **66**, 112-119.

Zhi, Y., Jia, G., Gerelchimeg, B., Shi-chao, L., Yan-shuang, M. and Zhong-hua, L. (2014). Lentivirus Mediated Gene Manipulation in Trophectoderm of Porcine Embryos. *Journal of Northeast Agricultural University (English Edition)* **21**, 39-45.

Figures

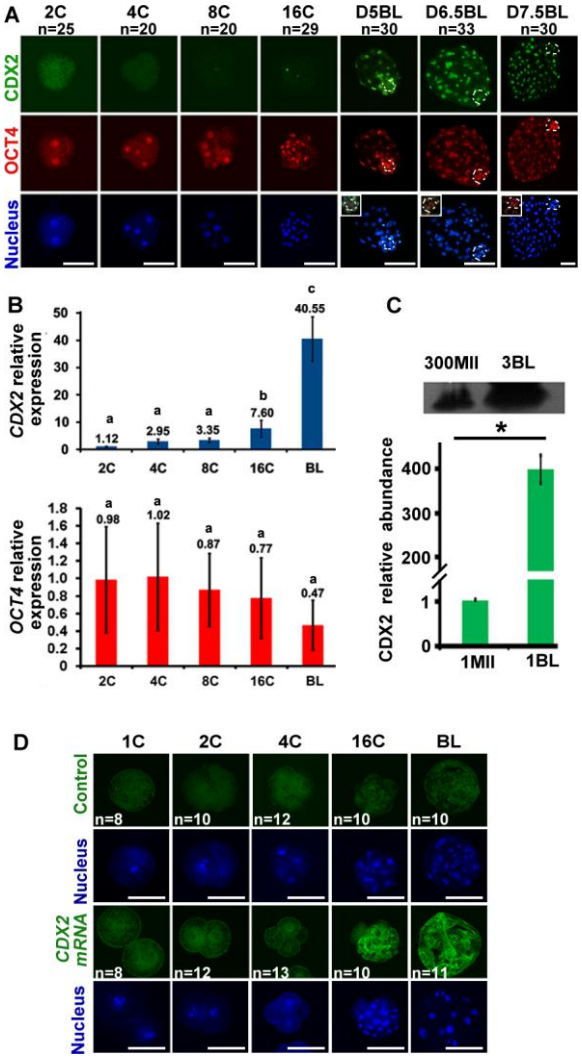

Fig. 1. Spatiotemporal expression pattern of *CDX2* in early stage porcine embryos. (A) Immunofluorescence (IF) images (epifluorescence microscope) for CDX2 and OCT4 expression at different developmental stages. Dashed lines indicate the ICM. "n": number of tested embryos. Merged images of ICM region are placed on the corner of last row images. (B) *CDX2* and *OCT4* mRNA expression level relative to their MII stage expression level (set as 1). Data indicate mean± SD (6 technical replicates).

Different characters (a, b, c) above bars indicate significant difference at $p<0.05$ using one-way ANOVA with Turkey's post hoc testing. (C) Western Blot (WB) analysis for CDX2 protein in 300 MII stage oocytes and three blastocysts. CDX2 protein abundances per MII stage oocyte and per D6 blastocyst are compared in the bar chart. * $p<0.05$. (D) RNA-FISH for *CDX2* in early stage porcine embryos. Sense mRNA of *CDX2* was used as a probe in control group. MII: MII stage porcine oocytes; BL: blastocyst. "n": number of tested embryos. Scale bars, 50μm.

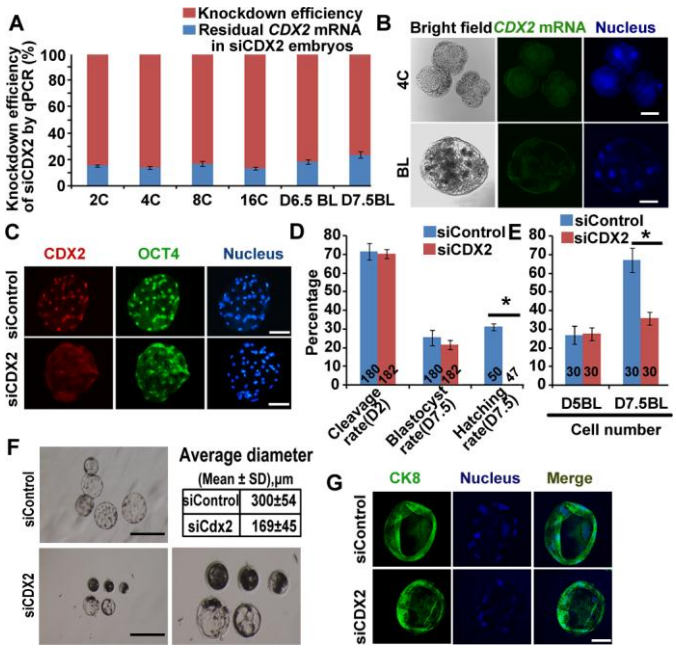

Fig. 2. The effects of *CDX2* knockdown on early porcine embryonic development. (A) qPCR was used to confirm *CDX2* knockdown in all embryonic stages examined. (B) RNA-FISH for CDX2 after siRNA injection. The images of paralleled control groups are shown in Fig.1D. Scale bar, 50μm. (C) IF assay compared CDX2 and OCT4 expression in D6.5 siCDX2 (n=15) and siControl (n=12) blastocysts. Scale bar, 50μm. (D) Developmental rates of siCDX2 and siControl embryos. Data on bars indicates the total number of embryos analyzed. * $p<0.05$. (E) Cell numbers in D5 and 7.5 siCDX2 and siControl blastocysts. Data on bars indicates the total number of embryos analyzed. * $p<0.05$. (F) The morphologies and diameters of D7.5 siCDX2 and siControl blastocysts. Scale bar, 500μm. (G) Sectional confocal images of CK8 in D7.5 siCDX2 (n=15) and siControl (n=15) blastocysts. Scale bar, 50μm.

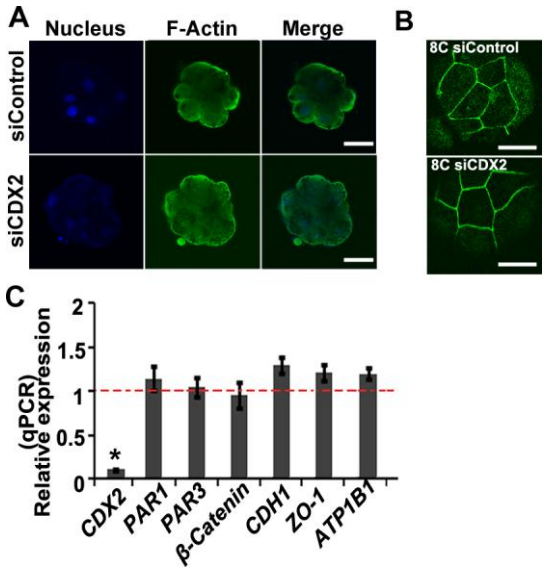

Fig. 3. CDX2 is dispensable to the polarization and junctions in cleavage stages porcine embryos. (A) Sectional confocal images of F-actin in siCDX2 (n=10) and siControl (n=8) 8-cell stage embryos. Scale bar, 50μm. (B) Sectional confocal images of E-cadherin IF staining in siCDX2 (n=12) and siControl (n=10) 8-cell stage embryos. Scale bar, 50μm. (C) qPCR analysis of *CDX2*, *PAR1*, *PAR3*, *CTNNB1*, *CDH1*, *ZO1*, and *ATP1B1* in siCDX2 8-cell stage embryos. Data indicate $2^{-\Delta\Delta Ct}$±SD (3 technical replicates). The expression levels in siControl embryos are set as 1 (red line). * indicates significant difference ($p<0.05$).

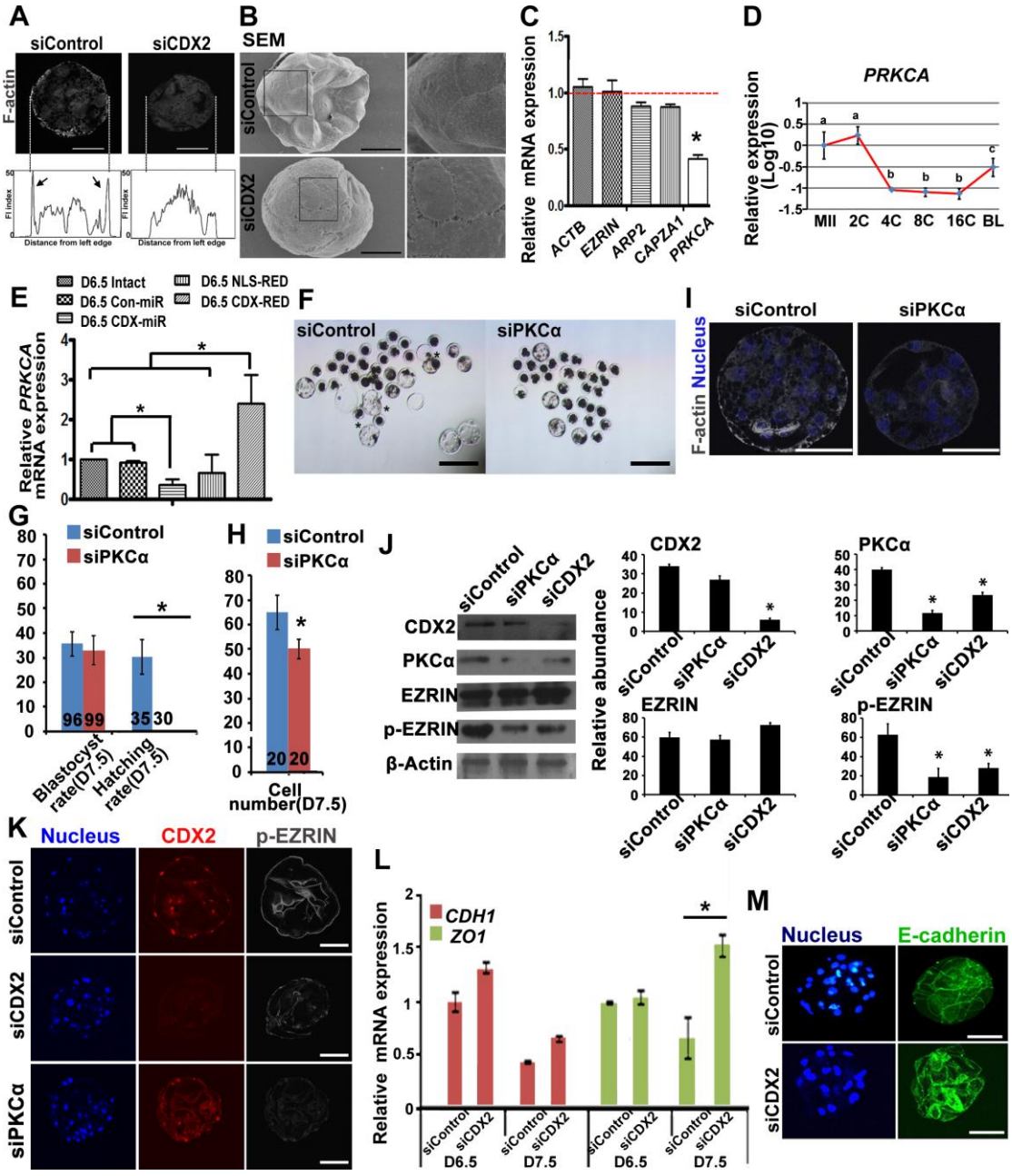

Fig. 4. CDX2 is essential for maintaining cell polarity of TE via regulation of PKCα expression. (A) Immunostaining F-actin of D6.5 siCDX2 (n=12) and siControl (n=13) blastocysts. TE cells in siCDX2 blastocysts lack apical F-actin. Below the IF images, the corresponding fluorescence intensities (FI) from left middle point to right middle point are plotted (Image J software). The arrows on plots indicate the apical polarization of F-actin in siControl blastocysts. (B) The status of superficial microvilli of D6.5 siCDX2 and siControl blastocysts was examined by SEM. (C) qPCR analysis of genes related to microvilli

formation in siCDX2 blastocysts. The values indicate $2^{-\Delta\Delta Ct}$±SD. (3 technical replicates). Gene expression in siControl embryos were set as 1 (red line).* $p<0.05$. (D) qPCR analysis of *PRCKA* in preimplantation porcine embryos. Different characters (a, b, c) on bars indicate significant difference ($p<0.05$). (E) qPCR analysis of *PRKCA* expression in TE specific *CDX2* regulated D6.5 porcine embryos. Intact: uninfected control, Con-miR: infected with virus expressing negative control miRNA, CDX-miR: infected with virus expressing CDX2 miRNA, NLS-RED: infected with virus expressing nonfunctional, nuclear localizing fluorescent protein, CDX-RED: infected with virus expressing fluorescent protein tagged CDX2. * $p<0.05$. (F) Hatching failure of siPKCα embryos. (* designates hatched control blastocysts, Scale bar, 500μm). (G) Developmental rate of siPKCα and siControl embryos. (H) Cell number of D7.5 siPKCα and siControl blastocysts. In G, H, the numbers shown on bars indicates the total number of embryos analyzed. * $p<0.05$. (I) Sectional confocal image indicated the loss of polarized F-actin in siPKCα embryos. (J) WB images and quantification of the CDX2, PKCα, EZRIN and phosphorylated EZRIN protein levels in siCDX2, siPKCα, and siControl blastocysts. The protein extract of 100 embryos were loaded per lane. (K) Sectional confocal images showed that p-EZRIN was down-regulated in D6.5 siCDX2 and siPKCα blastocysts. (L) qPCR analysis of *CDH1* and *ZO-1* expression in siCDX2 blastocysts relative to their expression in D6.5 siControl embryos. The values indicate $2^{-\Delta\Delta Ct}$± SD. (3 technical replicates). * $p<0.05$. (M) IF staining of E-cadherin shows a dispersed distribution in siCDX2 D6.5 blastocysts (n=8) compared with the siControl D6.5 blastocysts (n=10). Scale bar, 50μm.

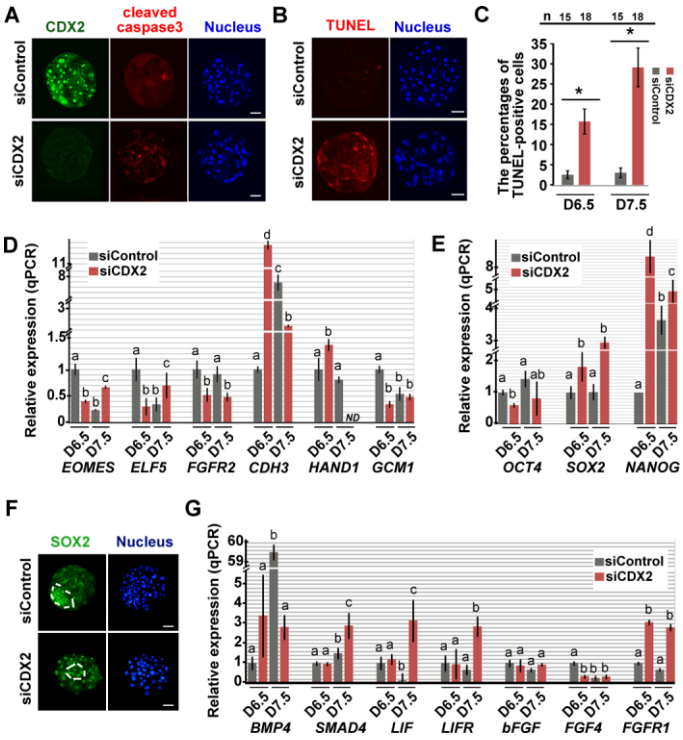

Fig. 5. *CDX2* knockdown increases apoptosis and disturbs genes expression in blastocysts. (A) Comparison of the confocal sectional images of cleaved caspase3 staining in D6.5 siCDX2 and siControl blastocyst. (B) TUNEL staining of D6.5 siCDX2 and siControl blastocysts. (C) The percentage of TUNEL-positive cells in D6.5 blastocysts. "n": number of embryos assayed. * $p<0.05$. (D) qPCR analysis of TE related genes. (E) qPCR analysis of ICM related genes. (F) Z-stack confocal images of SOX2 staining of D6.5 siCDX2 and siControl blastocysts. Dashed line indicates the ICM area. Scale bars: 50μm. (G) qPCR analysis of signaling pathway-related genes. In D, E and G, values are compared with the expression level in D6.5 siControl embryos and indicated as $2^{-\Delta\Delta Ct}$±SD (3 technical replicates), and the different characters (like a, d, c..) above bars indicate significant difference at $p<0.05$) using one-way ANOVA with Turkey's post hoc testing.

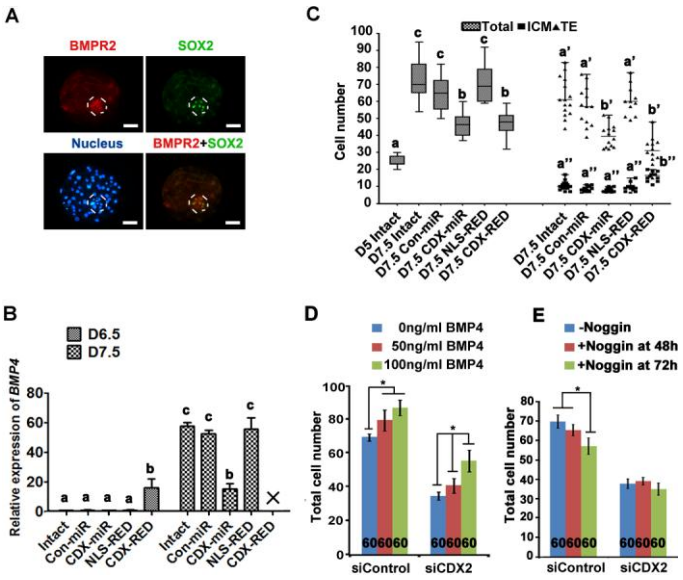

Fig. 6. CDX2 is crucial for blastocyst cell viability and proliferation via BMP4 signaling. (A) The images of epifluorescence microscope show that BMPR2 mainly expresses in ICM cells (SOX2-positive) of porcine blastocyst. The dashed line in images indicated the ICM. Scale bar, 50μm. (B) qPCR analysis of *BMP4* expression after lentivirus mediated TE-specific *CDX2* regulation. All values are compared with the expression in D6.5 intact embryos and indicated as $2^{-\Delta\Delta Ct}$±SD (3 technical replicates). Different characters (a, b, c) above bars indicate significant difference at $p<0.05$ using one-way ANOVA with Turkey's post hoc testing. Cross mark on the last bar indicates the embryonic degeneration of D7.5 CDX-RED embryos. (C) Box plot of total, ICM and TE cell numbers after TE-specific *CDX2* regulation. Different characters a, b, c (total), a', b', c' (TE), or a'', b'', c'' (ICM) above bars/plots indicate significant within-groups difference at $p<0.05$ using the one-way ANOVA with Kruskal–Wallis test with Dunn's correction. (D) Blastocyst cell numbers after treatment with different concentrations of BMP4. (E) Blastocyst cell numbers after 48 or 72 h treatment with BMP4 antagonist Noggin. In D and E, the numbers shown on bars indicates the total number of embryos tested; * $p<0.05$.

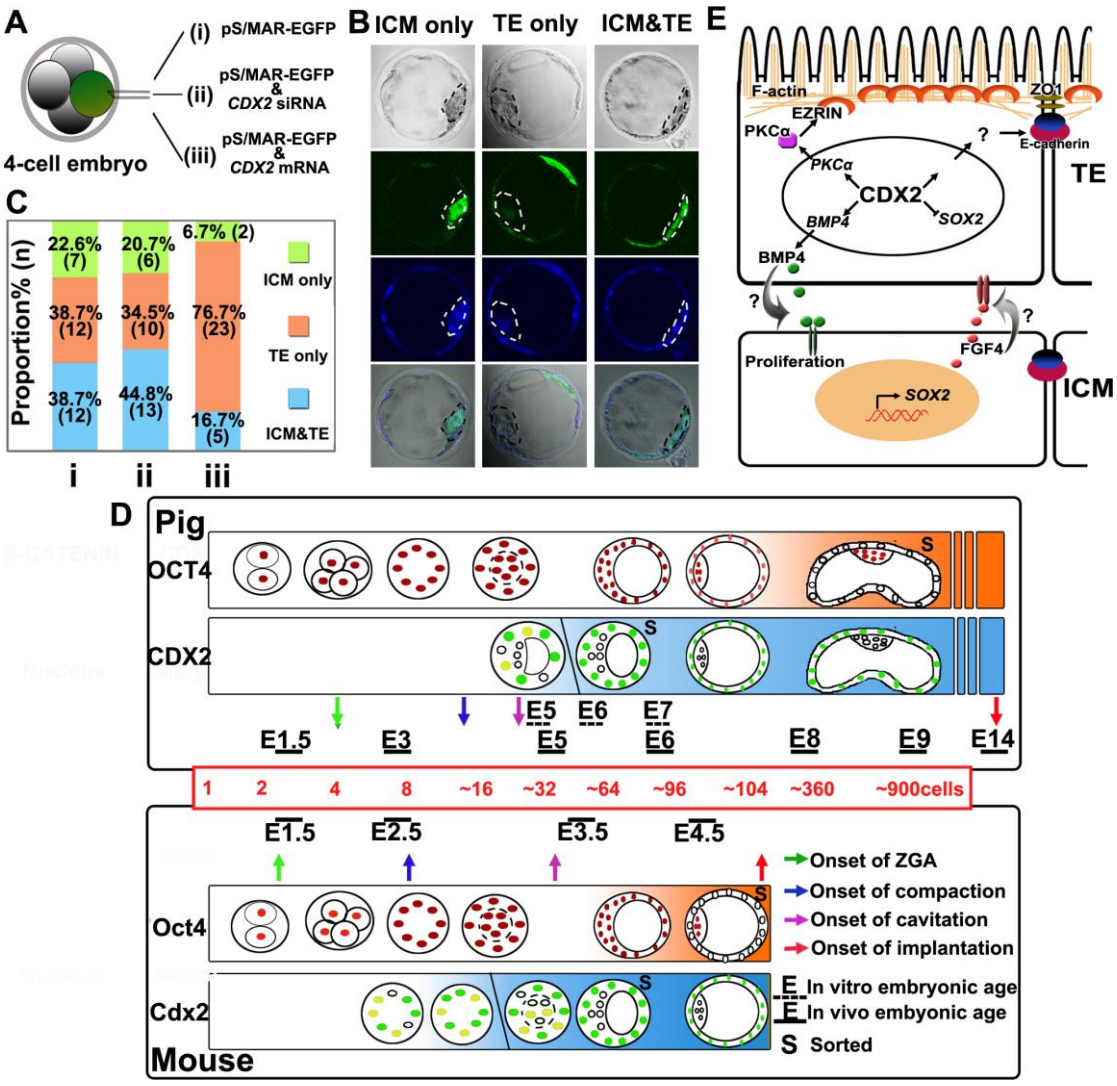

Fig. 7. *CDX2* up-regulation in early blastomeres causes a differentiation bias towards TE lineage. (A) Scheme for experimental strategy. (B) Representative confocal sectional images illustrate three groups of blastocysts. (C) The proportions of three type blastocysts in three experimental groups shown in A. The proportion and embryo numbers (in brackets) of every type are indicated on bars. (D) CDX2 and OCT4 expression pattern in early porcine and mouse embryos (modified based on the mouse pattern in previous literature (Dietrich and Hiiragi, 2007)). Green or dark red represent strong expression, yellow or light red represent weak expression and empty circles absence of nuclear CDX2 or OCT4. (E) Schematic summary of CDX2 functions in porcine blastocysts.

Supplementary Information

Supplementary Figures:

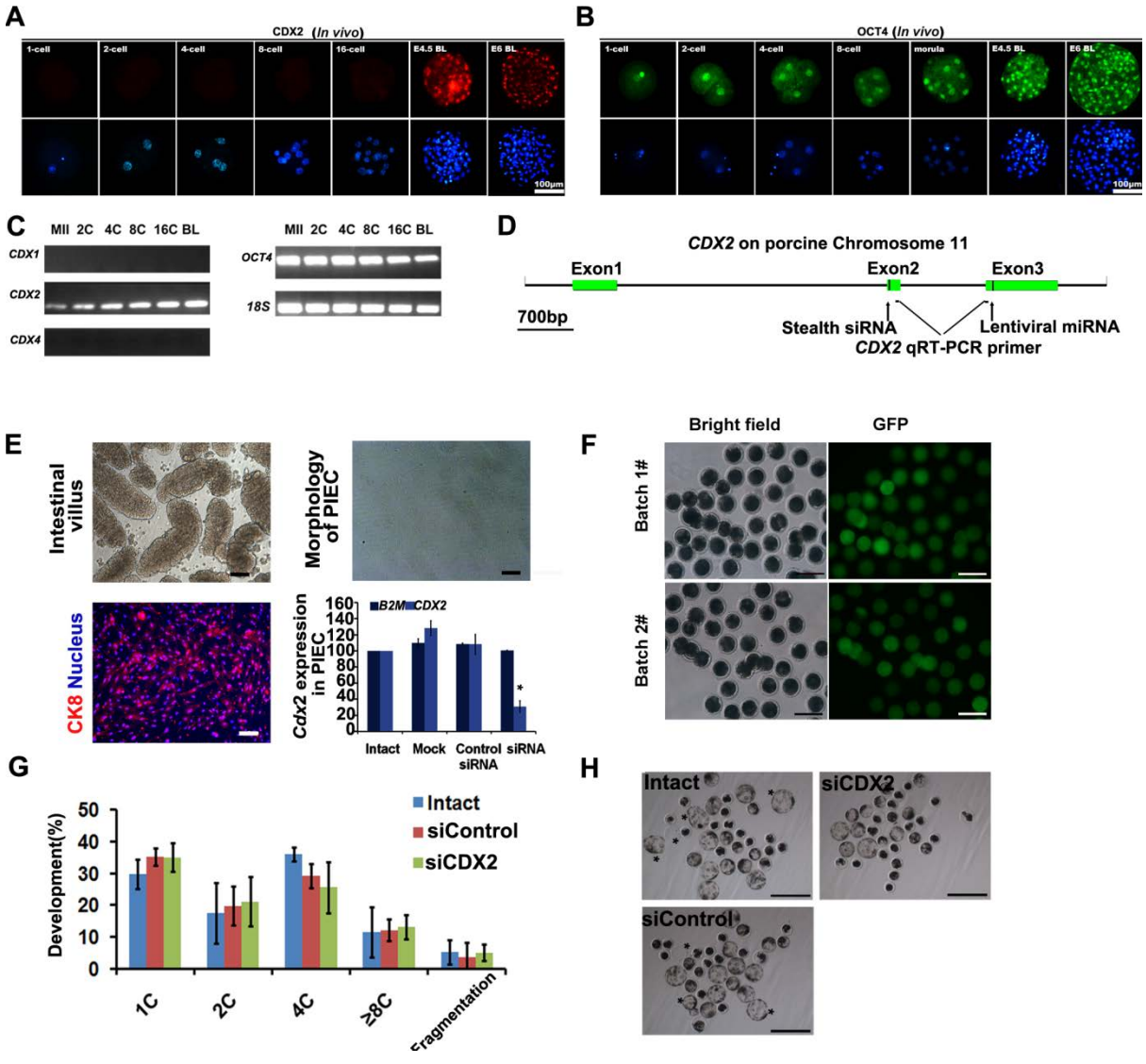

Fig. S1 The effects of *CDX2* knockdown on porcine embryonic development. (A-B) IF assays shows the *in vivo* expression pattern of (A) OCT4 (green) and (B) CDX2 (red). (C) RT-PCR proved the *CDX2* and *OCT4* mRNA expression throughout the development and the absence of *CDX1* and *CDX4* expression in porcine early stage embryos. (D) Illustration of locus targeted by CDX2 interfering tools and primers for qPCR. This study used two methods to knockdown *CDX2*: Stealth siRNA injection in zygotes and miRNA- expressing lentivirus mediated CDX2 knockdown. “Stealth siRNA” and “Lentiviral miRNA”

labeled their target locus. (E) Stealth siRNA also could effectively repress CDX2 expression in porcine intestinal epithelial cells (PIEC). Bar, 100μm. (F) Injection of GFP mRNA into porcine zygotes has shown that our injection efficiency is close to 100%. Bar, 100μm. (G) The morphology of embryos at D6.5. Bar, 500μm. (H) Embryonic development at D3.

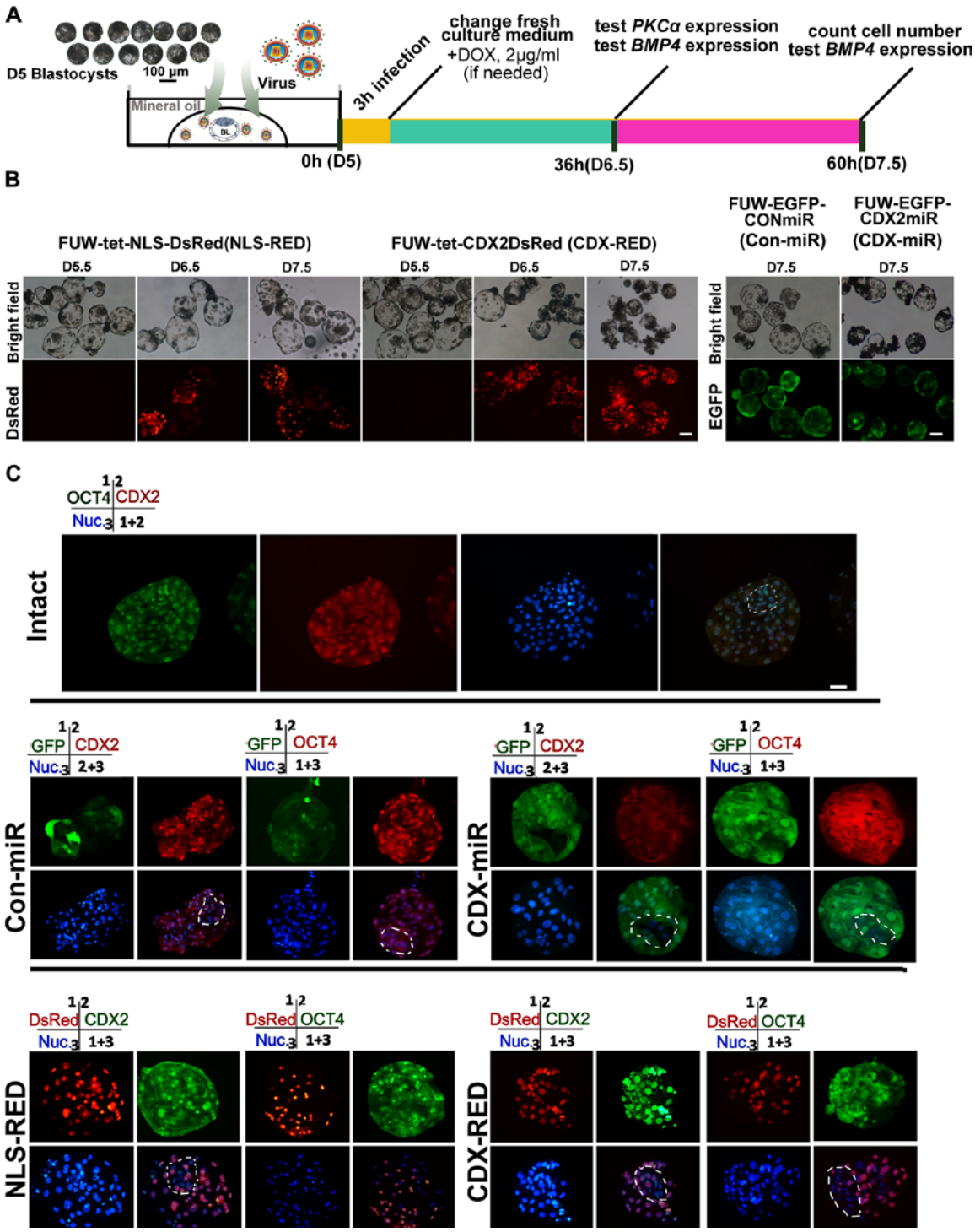

Fig. S2 Lentivirus mediated TE specific *CDX2* regulation. (A) The procedure of lentivirus infection and following experiments. (B) The status of blastocysts after lentivirus transfection. (C) IF assay shows the CDX2 and OCT4 expression after TE specific lentivirus infection. Bar, 50μm.

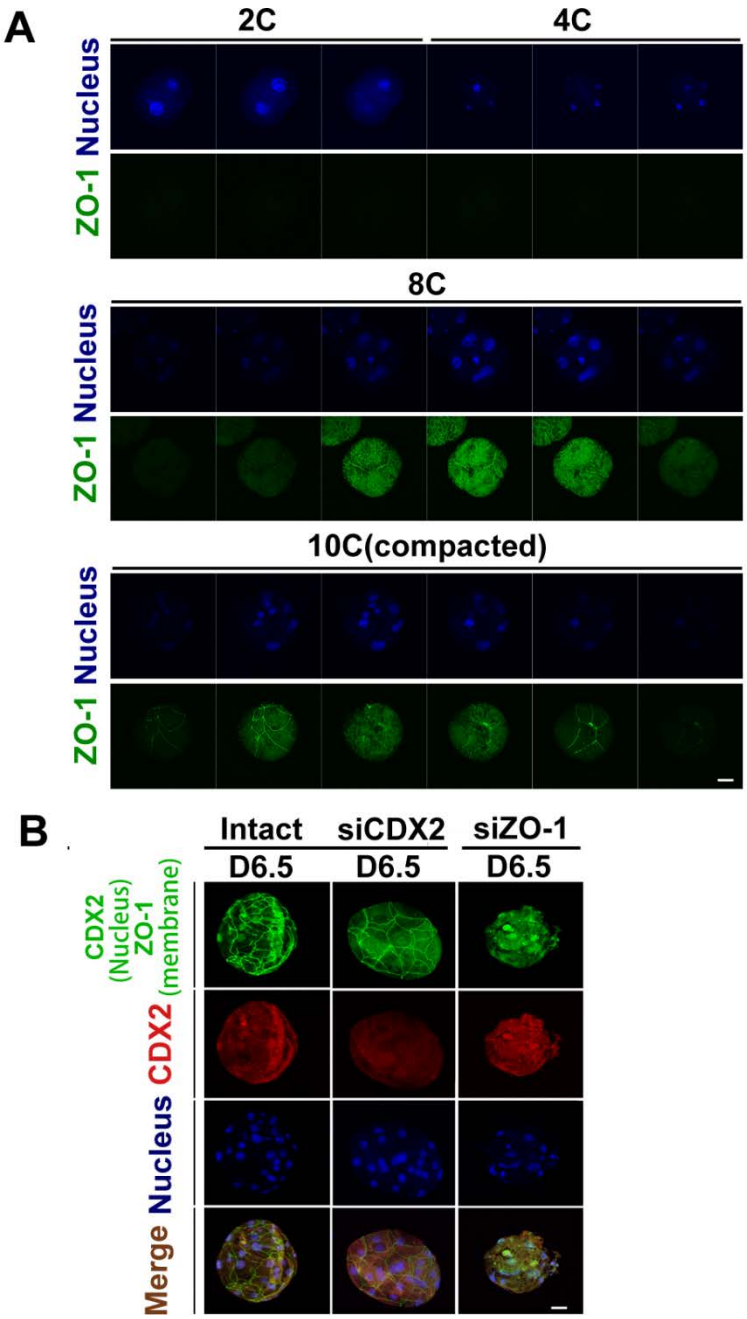

Fig. S3 CDX2 expression and the tight junction formation are independent events. (A) IF assay against ZO-1 in cleavage stage porcine embryos indicates that the formation of tight junction in porcine embryos is earlier than the CDX2 accumulation. (B) IF results show that the formation of tight junction (marked by ZO-1) and CDX2 expression are independent, because RNA interference against each of them does not affect the another one. Bar, 50μm.

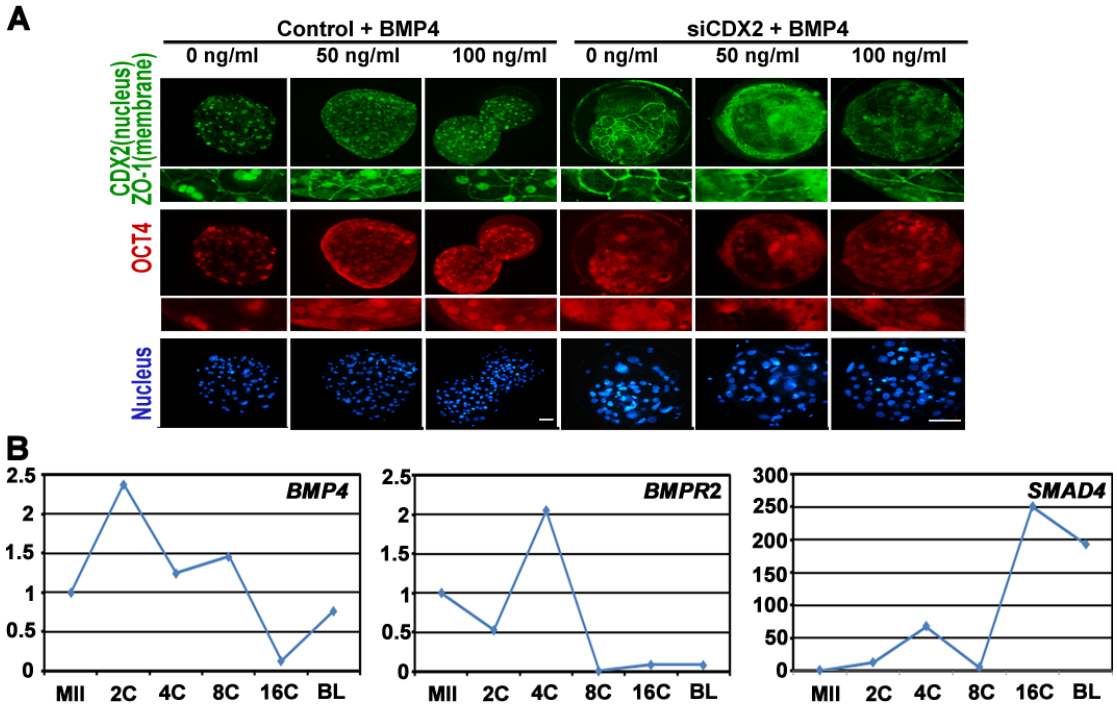

Fig. S4 BMP4 signaling is active in porcine blastocysts. (A) IF assay was used to calculate the blastocyst cell numbers after BMP4 supplement and at the same time prove CDX2 absence in siCDX2 blastocysts. Bar, 50μm. (B) The mRNA expression patterns of *BMP4*, *Smad4* and *BMPR2* throughout early porcine embryo.

Supplementary Tables:

Table S1. Primers used for qPCR

Gene	GeneBank No.(Ensemble ID)	Primer pairs
CDX2	AM778830	F: 5'AGTCGCTACATCACCATTCGGAG3' R: 5'GCTGCTGTTGCTGCAACTTCTTC3 '
POU5F1	NM_001113060	F: 5'GAAGCTGGACAAGGAGAAGCTGGAG3 ' R: 5'ATGGTCGTTTGGCTGAACACCTTC3 '
NANOG	AY596464	F: 5'CCTCCATGGATCTGCTTATTC3 ' R: 5'CATCTGCTGGAGGCTGAGGT 3 '
SOX2	NM_001123197	F: 5'AACCAGAAGAACAGCCCAGAC3 ' R: 5'TCCGACAAAAGTTTCCACTCG3 '
GATA4	NM_214293	F: 5'ATGAAGCTCCATGGTGTCCC 3 ' R: 5'ACTGCTGGAGTTGCTGGAAG3 '
GATA6	NM_214328	F: 5'TTGGTTATTCCCGAATTTCTCCG3 ' R: 5'CATTCCTGCAAACTGGGTGATAC3 '
CDH1	NM_001163060.1	F: 5'TGCTGCTCCTGCTCCTTATTCG3 ' R: 5'CTGGTCCTCTTCTCCACCTCCT3 '
ZO-1	AJ318101.1	F: 5'AGTGGCGTTGACACGTTCTCTG3 ' R: 5'ACCACGGTGTGACCATCCTCAT3 '
PRKCA	XM_005668672.1	F: 5'GGAGACAGCCTTCCAACAACCT3 ' R: 5'TGTCGGCGAGCATCACCTTC3 '
ATP1B1	AJ401029.1	F: 5'TGTGCCCAGCGAACTCAAAGAA3 ' R: 5'CCAACCATTCGAGCCTGAACCT3 '
EOMES	XM_003132081.2	F: 5'TGGACTCAATCCTACTGCCCACTAC3 ' R: 5'TTTGCCGCAGGTCACCCACTT3 '
ELF5	NM_001243711.1	F: 5'TCCTCCAGAACATTCGCTCACAAG3 ' R: 5'TGATGAGAACTTTGGAGGCTTGTTC3 '
CDH3	（ENSSSCT00000026686.1）	F: 5'GTCACAGACCAGAACGACCACAAG3 ' R: 5'CATCGTCCTCATCGGTGGCTGT3 '
HAND1	NM_001014428.1	F: 5'CCGAGCTGCGCGAGTGCAT3 ' R: 5'TTGGCCAGCACGTCCATCAGGT3 '
GCM1	XM_001927486.5	F: 5'CCTTTCTCCTCACCTATACCTCTC3 ' R:

Table S2. Antibodies Used for IF and WB assays

Primary antibody			
Immunogen	Source	Dilution	Description
a peptide mapping near the N-terminus of Oct-3/4 of human origin	sc-8628 Santa Cruz	IF:1:50	OCT4, Goat polyclonal IgG
human CDX2 recombinant protein	ab-88129 Abcam	IF:1:50 WB:1:500	CDX2, Rabbit monoclonal IgG
Human E-Caherin	ab-1416 Abcam	IF:1:50	E-CADHERIN, Mouse monoclonal IgG1
Human ZO-1	339188 Invitrogen	IF:1:500	Mouse monoclonal antibody conjugated to Alexa Fluor 488
A synthetic peptide corresponding to internal region of human NANOG	PAB6837 Abnova	IF:1:50	NANOG, Goat polyclonal
a peptide mapping near the C-terminus of Sox-2 of human origin	sc-17320 Santa Cruz	IF:1:100	SOX2, Goat polyclonal IgG
peptide region of the Human ZFP42 protein sequence according to NP_777560	SAB2102769 Sigma	IF:1:100	ZFP42(REX1), Rabbit polyclonal
Human Cytokeratin-18	BM0032 Boster	IF:1:100	CK8, Mouse monoclonal IgG
a peptide from the p17 fragment corresponding to the cleaved region of caspase-3 human caspase-3	G7481 Promega	IF:1:500	Active- CASPASE3, Rabbit polyclonal
synthesized peptide derived from human Catenin-β	SAB4500543 Sigma	IF:1:100	endogenous levels of total CATNB (Catenin-β), Rabbit polyclonal IgG
the C-terminus of PKC ζ of rat origin	sc-216 Santa Cruz	IF:1:50	PKCζ, Rabbit polyclonal IgG
residues surrounding Thr567 of human ezrin,	3149P CST	IF:1:500 WB:1:1000	Phospho-Ezrin (Thr567), Rabbit monoclonal IgG
amino acids 311-586 mapping at the C-terminus of human Ezrin	sc-20773 Santa Cruz	IF:1:500 WB:1:1000	Total Ezrin, Rabbit polyclonal IgG
the C-terminus of PKCα of human origin	sc-208 Santa Cruz	IF:1:500 WB:1:100	PKCα, Rabbit polyclonal IgG

Secondary antibody	
Name	Source
Alexa Fluor 546 Donkey Anti-Rabbit IgG	Molecular Probe A10040
Alexa Fluor 546 Donkey Anti-Mouse IgG	Molecular Probe A10036
Alexa Fluor 546 Donkey Anti-Goat IgG (H+L)	Molecular Probe A11056
Alexa Fluor 488 Donkey Anti-Goat IgG (H+L)	Molecular Probe A11055
Alexa Fluor 488 Doncky Anti-Rabbit IgG (H+L)	Molecular Probe A21206
Alexa Fluor 488 Donkey Anti-Mouse IgG (H+L)	Molecular Probe A21202
Anti-Rabbit IgG (whole molecule) –Peroxidase antibody produced in goat	Sigma A9169
Anti-Mouse IgG (whole molecule) –Peroxidase antibody produced in rabbit	Sigma A9044

Note Commercial antibodies have been tested and found to not work in pig including :

OCT4: sc-8629 Santa Cruz; O8389 Sigma
CDX2: AB4123 Millipore; 3977S Cell Signaling
NANOG: sc-33760 Santa Cruz; ab21624 Abcam
SOX2: ab97959 Abcam
ZFP42: ab50828 Abcam

Supplementary Information

Supplementary Figures:

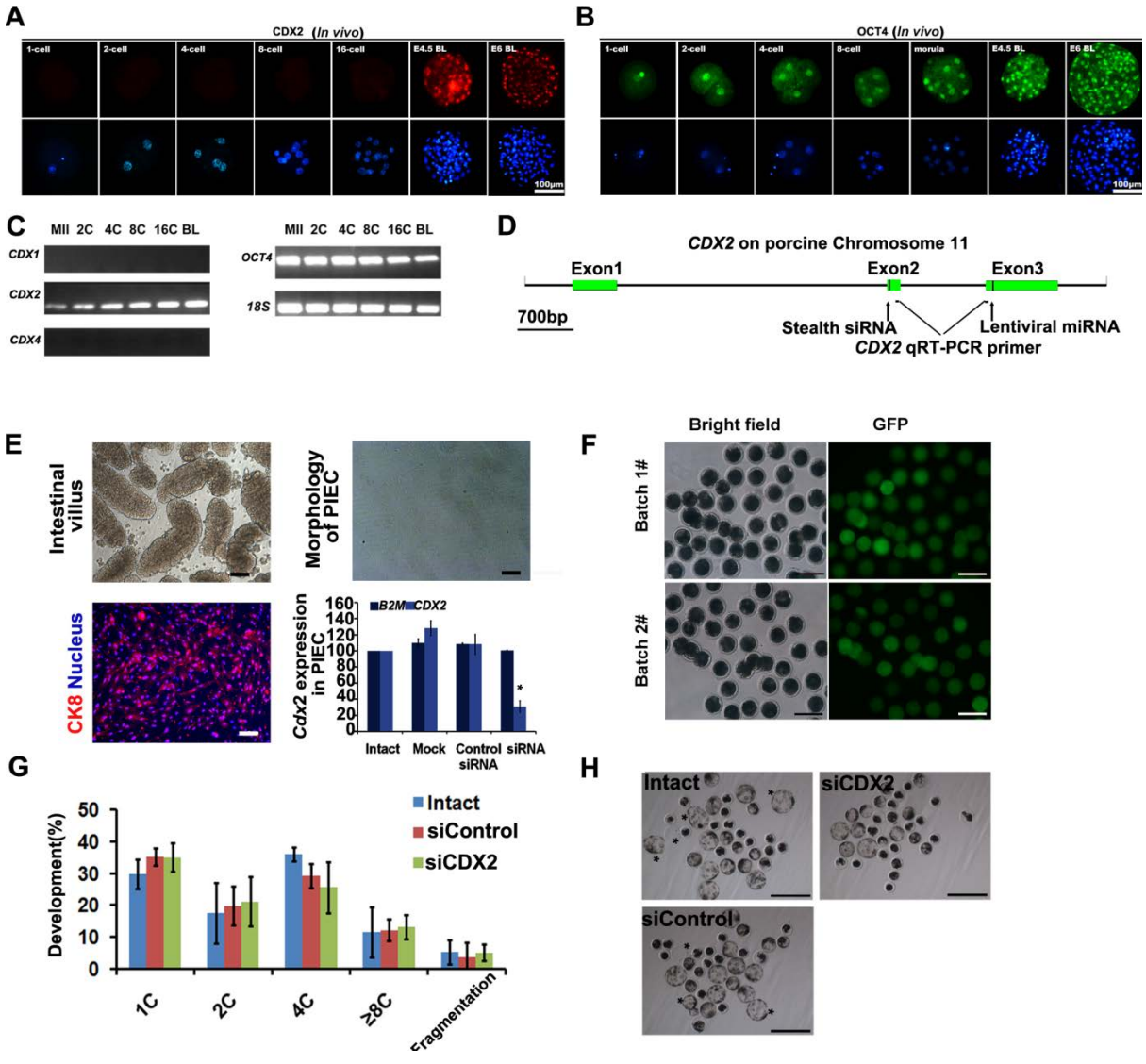

Fig. S1 The effects of *CDX2* knockdown on porcine embryonic development. (A-B) IF assays shows the *in vivo* expression pattern of (A) OCT4 (green) and (B) CDX2 (red). (C) RT-PCR proved the *CDX2* and *OCT4* mRNA expression throughout the development and the absence of *CDX1* and *CDX4* expression in porcine early stage embryos. (D) Illustration of locus targeted by CDX2 interfering tools and primers for qPCR. This study used two methods to knockdown *CDX2*: Stealth siRNA injection in zygotes and miRNA- expressing lentivirus mediated CDX2 knockdown. “Stealth siRNA” and “Lentiviral miRNA”

labeled their target locus. (E) Stealth siRNA also could effectively repress CDX2 expression in porcine intestinal epithelial cells (PIEC). Bar, 100μm. (F) Injection of GFP mRNA into porcine zygotes has shown that our injection efficiency is close to 100%. Bar, 100μm. (G) The morphology of embryos at D6.5. Bar, 500μm. (H) Embryonic development at D3.

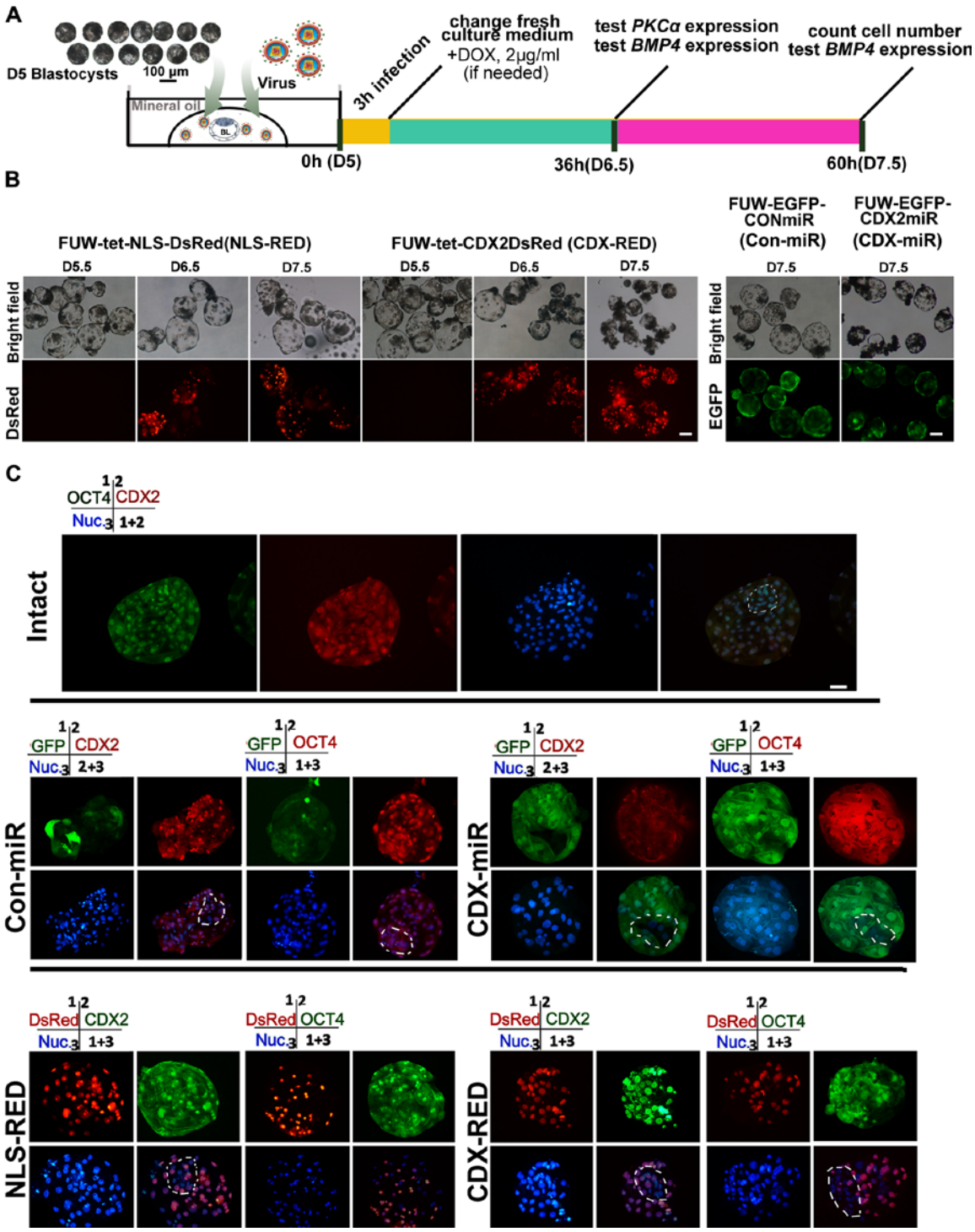

Fig. S2 Lentivirus mediated TE specific *CDX2* regulation. (A) The procedure of lentivirus infection and following experiments. (B) The status of blastocysts after lentivirus transfection. (C) IF assay shows the CDX2 and OCT4 expression after TE specific lentivirus infection. Bar, 50μm.

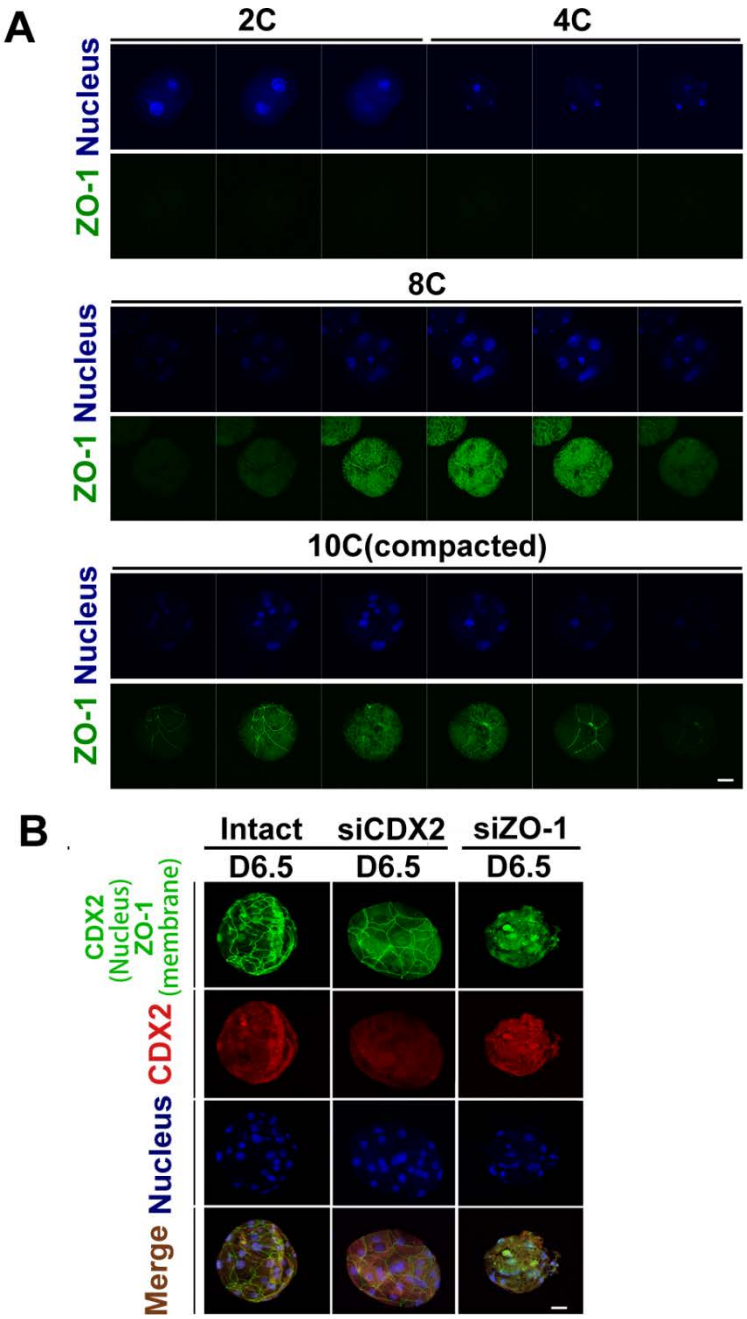

Fig. S3 CDX2 expression and the tight junction formation are independent events. (A) IF assay against ZO-1 in cleavage stage porcine embryos indicates that the formation of tight junction in porcine embryos is earlier than the CDX2 accumulation. (B) IF results show that the formation of tight junction (marked by ZO-1) and CDX2 expression are independent, because RNA interference against each of them does not affect the another one. Bar, 50μm.

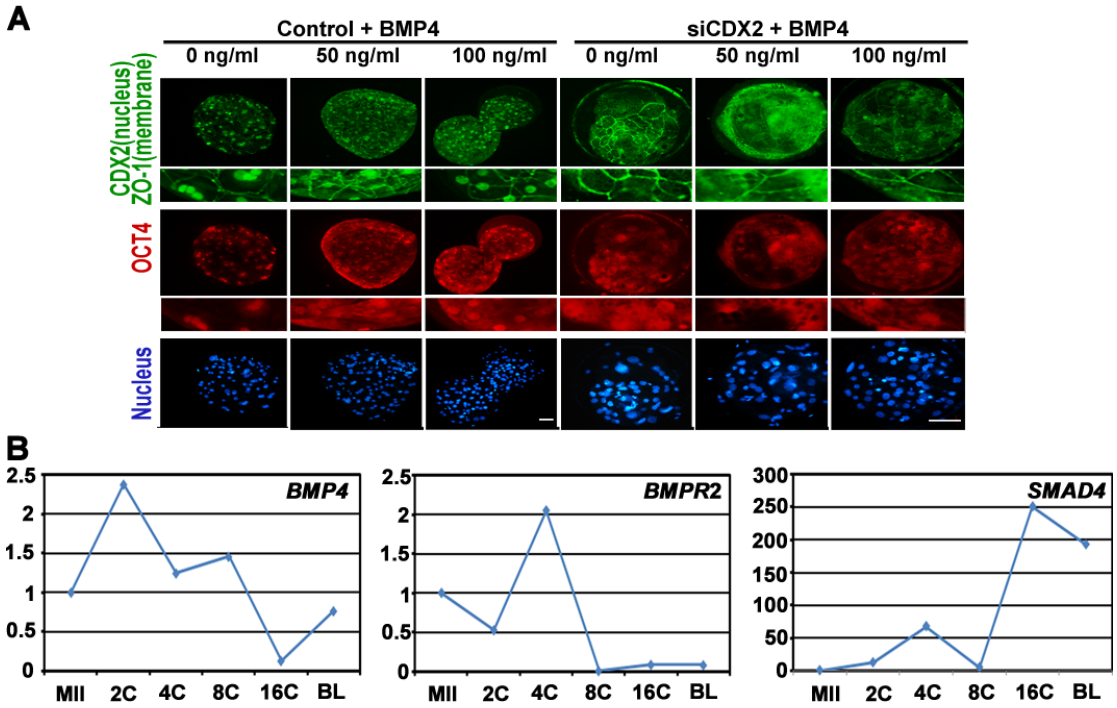

Fig. S4 BMP4 signaling is active in porcine blastocysts. (A) IF assay was used to calculate the blastocyst cell numbers after BMP4 supplement and at the same time prove CDX2 absence in siCDX2 blastocysts. Bar, 50μm. (B) The mRNA expression patterns of *BMP4*, *Smad4* and *BMPR2* throughout early porcine embryo.

Supplementary Tables:

Table S1. Primers used for qPCR

Gene	GeneBank No.(Ensemble ID)	Primer pairs
CDX2	AM778830	F: 5'AGTCGCTACATCACCATTCGGAG3' R: 5'GCTGCTGTTGCTGCAACTTCTTC3 '
POU5F1	NM_001113060	F: 5'GAAGCTGGACAAGGAGAAGCTGGAG3 ' R: 5'ATGGTCGTTTGGCTGAACACCTTC3 '
NANOG	AY596464	F: 5'CCTCCATGGATCTGCTTATTC3 ' R: 5'CATCTGCTGGAGGCTGAGGT 3 '
SOX2	NM_001123197	F: 5'AACCAGAAGAACAGCCCAGAC3 ' R: 5'TCCGACAAAAGTTTCCACTCG3 '
GATA4	NM_214293	F: 5'ATGAAGCTCCATGGTGTCCC 3 ' R: 5'ACTGCTGGAGTTGCTGGAAG3 '
GATA6	NM_214328	F: 5'TTGGTTATTCCCGAATTTCTCCG3 ' R: 5'CATTCCTGCAAACTGGGTGATAC3 '
CDH1	NM_001163060.1	F: 5'TGCTGCTCCTGCTCCTTATTCG3 ' R: 5'CTGGTCCTCTTCTCCACCTCCT3 '
ZO-1	AJ318101.1	F: 5'AGTGGCGTTGACACGTTCTCTG3 ' R: 5'ACCACGGTGTGACCATCCTCAT3 '
PRKCA	XM_005668672.1	F: 5'GGAGACAGCCTTCCAACAACCT3 ' R: 5'TGTCGGCGAGCATCACCTTC3 '
ATP1B1	AJ401029.1	F: 5'TGTGCCCAGCGAACTCAAAGAA3 ' R: 5'CCAACCATTCGAGCCTGAACCT3 '
EOMES	XM_003132081.2	F: 5'TGGACTCAATCCTACTGCCCACTAC3 ' R: 5'TTTGCCGCAGGTCACCCACTT3 '
ELF5	NM_001243711.1	F: 5'TCCTCCAGAACATTCGCTCACAAG3 ' R: 5'TGATGAGAACTTTGGAGGCTTGTTC3 '
CDH3	（ENSSSCT00000026686.1）	F: 5'GTCACAGACCAGAACGACCACAAG3 ' R: 5'CATCGTCCTCATCGGTGGCTGT3 '
HAND1	NM_001014428.1	F: 5'CCGAGCTGCGCGAGTGCAT3 ' R: 5'TTGGCCAGCACGTCCATCAGGT3 '
GCM1	XM_001927486.5	F: 5'CCTTTCTCCTCACCTATACCTCTC3 ' R:

Table S2. Antibodies Used for IF and WB assays

Primary antibody			
Immunogen	Source	Dilution	Description
a peptide mapping near the N-terminus of Oct-3/4 of human origin	sc-8628 Santa Cruz	IF:1:50	OCT4, Goat polyclonal IgG
human CDX2 recombinant protein	ab-88129 Abcam	IF:1:50 WB:1:500	CDX2, Rabbit monoclonal IgG
Human E-Caherin	ab-1416 Abcam	IF:1:50	E-CADHERIN, Mouse monoclonal IgG1
Human ZO-1	339188 Invitrogen	IF:1:500	Mouse monoclonal antibody conjugated to Alexa Fluor 488
A synthetic peptide corresponding to internal region of human NANOG	PAB6837 Abnova	IF:1:50	NANOG, Goat polyclonal
a peptide mapping near the C-terminus of Sox-2 of human origin	sc-17320 Santa Cruz	IF:1:100	SOX2, Goat polyclonal IgG
peptide region of the Human ZFP42 protein sequence according to NP_777560	SAB2102769 Sigma	IF:1:100	ZFP42(REX1), Rabbit polyclonal
Human Cytokeratin-18	BM0032 Boster	IF:1:100	CK8, Mouse monoclonal IgG
a peptide from the p17 fragment corresponding to the cleaved region of caspase-3 human caspase-3	G7481 Promega	IF:1:500	Active- CASPASE3, Rabbit polyclonal
synthesized peptide derived from human Catenin-β	SAB4500543 Sigma	IF:1:100	endogenous levels of total CATNB (Catenin-β), Rabbit polyclonal IgG
the C-terminus of PKC ζ of rat origin	sc-216 Santa Cruz	IF:1:50	PKCζ, Rabbit polyclonal IgG
residues surrounding Thr567 of human ezrin,	3149P CST	IF:1:500 WB:1:1000	Phospho-Ezrin (Thr567), Rabbit monoclonal IgG
amino acids 311-586 mapping at the C-terminus of human Ezrin	sc-20773 Santa Cruz	IF:1:500 WB:1:1000	Total Ezrin, Rabbit polyclonal IgG
the C-terminus of PKCα of human origin	sc-208 Santa Cruz	IF:1:500 WB:1:100	PKCα, Rabbit polyclonal IgG

Secondary antibody	
Name	Source
Alexa Fluor 546 Donkey Anti-Rabbit IgG	Molecular Probe A10040
Alexa Fluor 546 Donkey Anti-Mouse IgG	Molecular Probe A10036
Alexa Fluor 546 Donkey Anti-Goat IgG (H+L)	Molecular Probe A11056
Alexa Fluor 488 Donkey Anti-Goat IgG (H+L)	Molecular Probe A11055
Alexa Fluor 488 Doncky Anti-Rabbit IgG (H+L)	Molecular Probe A21206
Alexa Fluor 488 Donkey Anti-Mouse IgG (H+L)	Molecular Probe A21202
Anti-Rabbit IgG (whole molecule) –Peroxidase antibody produced in goat	Sigma A9169
Anti-Mouse IgG (whole molecule) –Peroxidase antibody produced in rabbit	Sigma A9044

Note Commercial antibodies have been tested and found to not work in pig including :

OCT4: sc-8629 Santa Cruz; O8389 Sigma
CDX2: AB4123 Millipore; 3977S Cell Signaling
NANOG: sc-33760 Santa Cruz; ab21624 Abcam
SOX2: ab97959 Abcam
ZFP42: ab50828 Abcam